nature reviews earth & environment

https://doi.org/10.1038/s43017-023-00436-7

Review article

Check for updates

Southern Ocean glacial conditions and their influence on deglacial events

Elisabeth L. Sikes[1], Natalie E. Umling[1,2], Katherine A. Allen[3], Ulysses S. Ninnemann[4], Rebecca S. Robinson[5], Joellen L. Russell[6] & Thomas J. Williams[7,8]

Abstract

The Southern Ocean is an important regulator of global CO_2 levels and likely had a key role in lowering atmospheric CO_2 levels during the Last Glacial Maximum (LGM) and driving the subsequent increase during the following deglaciation. Nonetheless, debate continues surrounding the relative importance of Northern versus Southern Hemisphere forcing during deglacial events. In this Review, we compare modern Southern Ocean conditions with those in the LGM and deglacial period, identifying factors that were critical in initiating the glacial termination. During the LGM, North Atlantic sourced waters appear to have shoaled and were largely absent from the glacial Southern Ocean. Increased ocean stratification, shoaling of the chemical divide and increased nutrient utilization at the surface contributed to glacial carbon sequestration in deep waters. Warming at mid-latitudes of the Southern Hemisphere and the Southern Ocean began at ~21 ka, preceding deglaciation, indicating insolation changes could have driven early atmosphere–ocean warming that initiated the shifting of ocean fronts leading to the release of carbon sequestered in the LGM. Southern Ocean dynamics appear to have been substantial, or even the critical, factors initiating the termination of the LGM before deepening of North Atlantic sourced waters. Future research should focus on better resolving deglacial chemical and physical changes in Southern Ocean waters and their representation in numerical models.

Sections

Introduction

Modern Southern Ocean circulation

Southern Ocean dynamics during the LGM

Southern Ocean influences on deglaciation

Summary and future perspectives

A full list of affiliations appears at the end of the paper. e-mail: sikes@marine.rutgers.edu

Key points

- The Southern Ocean is where the major deep-water masses of oceans rise to the surface, mingle, modify and re-form, making it the nexus of global ocean interactions. Air–sea exchange of CO_2 in the Southern Ocean is a key control on atmospheric CO_2 concentrations, the marine carbon cycle and climate.
- During the Last Glacial Maximum (20–26 ka), North Atlantic sourced waters were largely absent from the glacial Southern Ocean. The likely cause of this is shoaling of North Atlantic Deep Waters to intermediate depths.
- The northern glacial Southern Ocean had a shallower and more intense geochemical divide than modern-day Southern Ocean. Increased ocean stratification, shoaling of the chemical divide and increased nutrient utilization at the surface contributed to glacial carbon sequestration in deep waters.
- Breakdown of the intensified geochemical divide and ventilation occurred early in the deglaciation, preceding the reintroduction of northern-sourced waters to the Southern Ocean.
- Shifts in Southern Hemisphere winds, frontal movements and orbital forcing could have driven these changes in Southern Ocean dynamics, triggering the release of carbon sequestered during the Last Glacial Maximum and increasing atmospheric CO_2 at the beginning of the deglaciation (~18-11 ka), affecting global climate.

Introduction

Ocean dynamics and circulation have a fundamental role in millennial-scale global carbon cycle and climate system feedbacks by regulating the amount of CO_2 in the atmosphere[1–6] and the distribution of heat between the hemispheres[3,7]. The Southern Ocean is where the major deep-water masses of oceans rise to the surface, mingle, modify and re-form, making it the nexus of global ocean interactions (Fig. 1) and an important area for ocean–atmosphere gas exchange[8–10]. The upwelling of deep waters provides nutrients to the surface of the Southern Ocean along with dissolved inorganic carbon (DIC), which was previously sequestered into the ocean interior allowing it to exchange with the atmosphere[11,12].

In addition to air–sea equilibration, uptake of carbon by photosynthesis and the export via sinking of organic matter into the deep ocean, termed the biological pump, act to decrease the surface DIC[13]. In the modern Southern Ocean, the upward supply of nutrients and DIC from deep waters outpace biological demand[14], resulting in an excess of unutilized nutrients and, crucially, carbon in surface waters that can exchange with the atmosphere as CO_2. The tight coupling and competition between these physical and biochemical carbon pumps determine the sign of the air–sea CO_2 fluxes. As the abyssal ocean waters rise to the surface in the Southern Ocean, this also impacts the ability of the deep ocean to retain carbon, giving the Southern Ocean an outsized role in the global carbon cycle.

The importance of Southern Ocean for carbon sequestration during the Last Glacial Maximum (LGM; ~21 ka)[15,16] and the subsequent carbon outgassing across the deglaciation (~18-11 ka) are widely recognized[3,17–22]. However, debate continues around the relative importance of Southern Ocean dynamics in comparison to those in the Northern Hemisphere. The Northern Hemisphere has long been considered the prime mover, determining the pace of glacial climate cycles. This thinking came about as the Northern Hemisphere is both the locus of continental glaciation and where the deep limb of the global overturning circulation initiates in North Atlantic.

However, the latest advances have revealed that the Southern Ocean preceded the North Atlantic in key deglacial responses. Initial warming in the Southern Ocean, which began around 21 ka, was earlier than the termination of the last Ice Age in the Northern Hemisphere and in the south, was accompanied by changes in sea-ice extent, frontal placement and deep ventilation that released deep sequestered CO_2 (refs. 21–25). As the Southern Ocean is crucial for setting the physical and chemical structure of the ocean, and thus the ability of the ocean to store CO_2, it follows that Southern Ocean processes were key drivers of the last deglaciation and changes in the ocean–atmosphere carbon partitioning that accompanied it[7,19,21,26–29]. Yet, quantifying the contribu-tions of Southern Ocean processes such as circulation, stratification, sea-ice extent, shifting wind belts and the biological pump to the rise in deglacial atmospheric CO_2 remains challenging.

In this Review, we explore Southern Ocean conditions and ocean–atmosphere interactions during the last glacial–deglacial transition and discuss the evidence suggesting that the Southern Ocean was critical in driving the termination of the LGM. We characterize the state of the glacial and deglacial Southern Ocean through discussion of published palaeoclimate proxy data and numerical simulations. We first examine the structure of the glacial Southern Ocean and the current under-standing of sea surface temperature (SST), the efficiency of biological processes, frontal placement, sea-ice extent, and winds, on oceanic overturning circulation and CO_2 sequestration. We then describe the deglacial changes in the same parameters and their association with millennial-scale climate events in the first half of the last degla-ciation. Temporally, we focus on Heinrich Stadial 1 (HS1; 14.5–17.5 ka) and the Antarctic Cold Reversal (ACR; 12.9–14.5 ka), to place empha-sis on the inception of the deglaciation. We chose this time period as later deglacial millennial events are not strongly expressed in the Southern Ocean. We discuss the evidence for early initiation of degla-ciation in the Southern Ocean, including two proposed mechanisms for how the Southern Hemisphere controls the progression of degla-ciation. We explore future research directions that will provide further insight into the role of the Southern Ocean in affecting the coupled ocean–atmosphere climate system.

Modern Southern Ocean circulation

The Southern Ocean serves as the conduit through which Atlantic, Indian and Pacific Ocean water masses are exchanged and modified[8,30]. Glacial and deglacial circulation in the Southern Ocean can be under-stood in reference to present-day circulation patterns. At present, deep Meridional Overturning Circulation (MOC) originates in the North Atlantic, with the thermohaline formation of North Atlantic Deep Water (NADW) that delivers a major component of northern-sourced waters to the deep Southern Ocean (Fig. 1). A distinct feature of modern circulation is that NADW is sufficiently dense to sit below the depth of the Drake Passage Sill allowing it to cross the geostrophic barrier formed by the circumglobal Antarctic Circumpolar Current (ACC)[8,31,32] and contribute to Lower Circumpolar Deep Water (Lower CDW)[8,33] (Box 1). Indian Deep Water and Pacific Deep Water are less dense than NADW and Lower CDW[34] and enter the Southern Ocean at a shallower depth (~1,600–3,000 m) forming the Upper Circumpolar

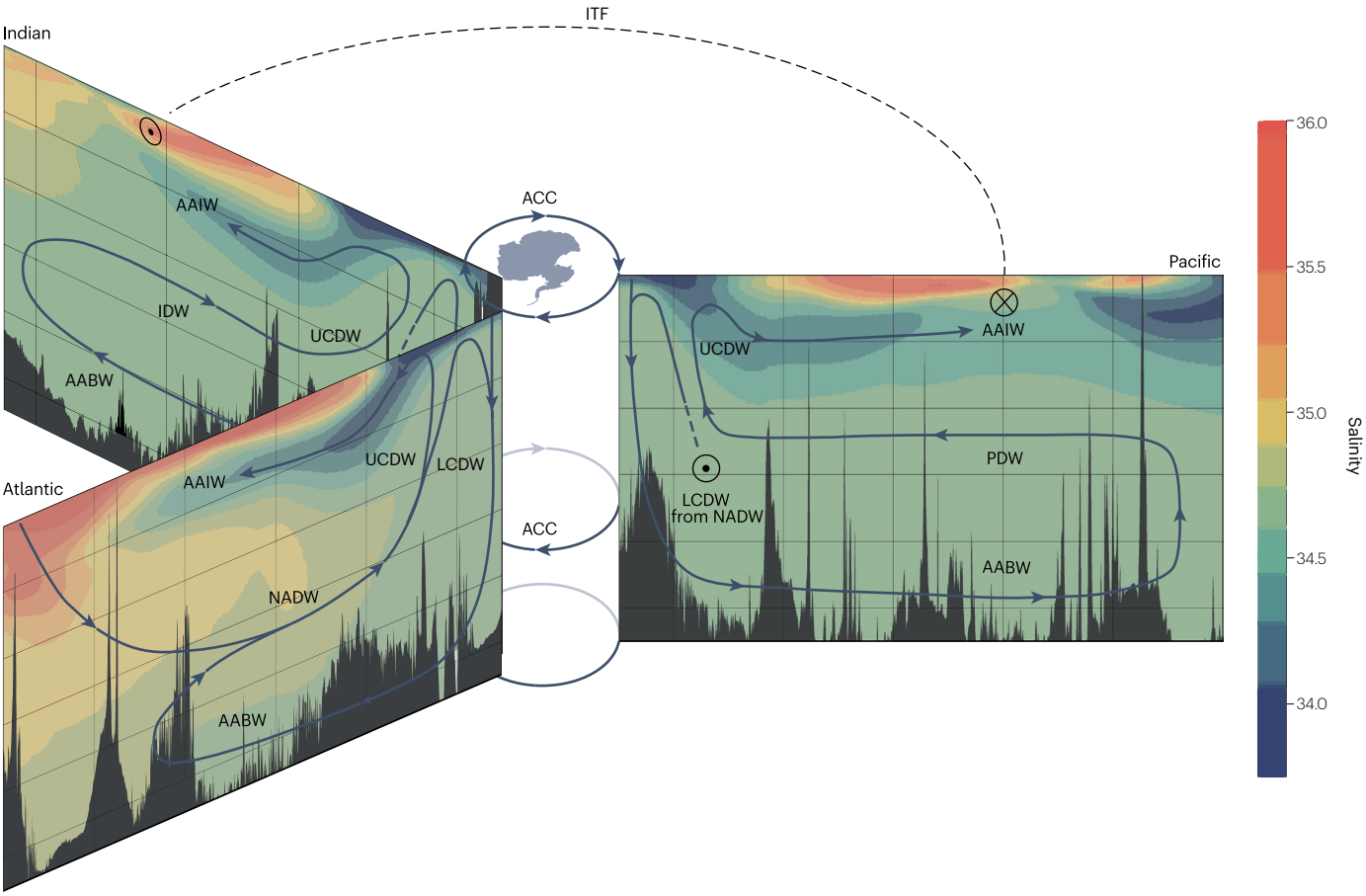

Fig. 1 | Global Meridional Overturning Circulation. Direction of flow is indicated by arrows, and salinity is indicated by colours. Major water masses abbreviated as: North Atlantic Deep Water (NADW), Indian Deep Water (IDW) and Pacific Deep Water (PDW) Antarctic Bottom Water (AABW). Southern Ocean water masses and currents: Lower Circumpolar Deep Water (LCDW), Upper Circumpolar Deep Water (UCDW), Antarctic Intermediate Water (AAIW), Antarctic Circumpolar Current (ACC). Other ocean currents: The Indonesian Throughflow (ITF). Bathymetry is displayed in black. Southern Ocean dynamics are where northern-sourced deep-water masses rise to the surface, mingle, modify and re-form, making it the nexus of global ocean interactions.

Deep Water (Upper CDW). Closure of the overturning circulation is intimately linked to the dynamics of the ACC and its eddy field that can carry mass and heat poleward[35] across the unbounded channel of the Southern Ocean at depths above bottom topography[36].

Southern Ocean water masses can be summarized as forming two overturning limbs derived from three layers. A mid-depth southward-flowing layer, sourced from NADW, Indian Deep Water (IDW) and Pacific Deep Water (PDW), transforms into two northward-flowing layers sitting above and below (Fig. 2). Sea-ice formation and cooling decrease the buoyancy of Lower CDW, leading to the formation of Antarctic Bottom Water (AABW), the densest, deepest, northward-flowing water mass. Farther north, Upper CDW freshens and gains buoyancy[37–41], forming Antarctic Intermediate Water (AAIW; 800–1,600 m) that subducts at the Subantarctic Front (SAF). Farther north, Subantarctic Mode Water (SAMW; 400–800 m) subducts at the Subtropical Front[8,42–46]. These waters form the upward limb of the thermohaline overturning circulation that ultimately flows northward (Fig. 2).

IDW and PDW, the source of Upper CDW, are relatively carbon-rich water masses. The upwelling of these waters to the surface primarily occurs in the turbulent winter through wind-driven deep mixing[44,45]. This wind-driven mixing causes SAMW and AAIW to exchange their CO_2 with the atmosphere while at the surface[8], thereby releasing sequestered carbon in excess of atmospheric levels which ventilates the water (Fig. 2). This ventilation occurs in distinct hot spots across the Southern Ocean largely driven by topography[44–46]. Equilibrium-driven exchange and loss of CO_2 to the atmosphere is a central factor in the atmosphere–ocean balance of CO_2 in the present day[12,45].

Fronts are important partitions and boundaries in the Southern Ocean, with the northern boundary of the Southern Ocean being the Subtropical Front. The fronts are steered by the winds[43] and the bathymetry that also direct the flow of the ACC[42,43,47] and drive the eddy mixing that provides closure of overturning circulation[35,48–50]. The response to topography[35,51] dictates that changes in the path of the ACC will affect dynamic balances, cross-front exchange[35,52] heat transport and shallow water mass formation[44]. Changes in ventilation and water mass formation can be expected to occur with climate-driven changes in frontal locations[35,53] and the path of the ACC with implications for the glacial state and deglacial response of the Southern Ocean.

Box 1

The Drake Passage, a gateway to the Southern Ocean for deep water

The Southern Ocean at the latitude of the Drake Passage (roughly 57°–61° S) is a circumglobal band of open sea through which the core of the Antarctic Circumpolar Current (ACC) flows (yellow arrow, see part **a** of the figure). This means that waters shallower than the sill depth (of about 2,500 m) lie on density surfaces (isopycnals) in the Drake Passage latitude band that are continuous all the way around Antarctica. These continuous isopycnals cannot support net east–west pressure gradients nor net meridional geostrophic flow. Waters that are denser and deeper can intersect the ocean bottom at a ridge, or sill, which can act as a deep meridional boundary, and therefore support a zonal pressure gradient and net north–south geostrophic flow. At present, global circulation forms one continuous overturning cell; North Atlantic Deep Water (NADW, green arrow, see the figure, part **a**) has a core density that matches or exceeds that found in the Drake Passage and so enters the Southern Ocean below ~ 2,000 m and upwells to the surface south of the ACC, where it becomes a source of Antarctic Bottom Water (AABW, dark blue arrow)[8,271]. Water on shallower isopycnals can only cross the ACC with the help of eddy-induced stirring that gradually mix across the ACC. The Pacific Ocean and the Indian Ocean do not have a northern source of deep water, but there is dynamic similarity, with each basin having deep water transport southward to where it rises to the surface in the Southern Ocean. Notably, Indian Deep Water (IDW) and Pacific Deep Water (PDW), which are lighter than the NADW, upwell in the Southern Ocean north of NADW where they are the main sources of the upper ocean waters that leave the Southern Ocean (Subantarctic Mode Water or SAMW, Antarctic Intermediate Water or AAIW)[8,10] (Fig. 1).

It is well established that NADW shoaled in the Last Glacial Maximum (and is commonly referred to as Glacial North Atlantic Intermediate water, GNAIW) putting most of the southward transport of Atlantic sourced waters at or above the Drake Passage sill depth (blue arrow, see the figure, part **b**). The dynamic constraints require that if NADW shoaled, this would require decreased densities that would have prevented these waters from entering the deep Southern Ocean. This would have restricted GNAIW transport to north of the ACC where through eddy closure they would have contributed to SAMW and AAIW, especially in the South Atlantic (see the figure, part **b**). In the South Atlantic, any non-obducted waters could have retroflected and contributed to a non-ventilated northern-source component observed at mid-depths[75]. In other basins, hypothetically, PDW and IDW would have filled the role of NADW during the Last Glacial Maximum (Fig. 2). If so, PDW and IDW would have outcropped south of the ACC supplying the waters that flowed southward to eventually form AABW. In the Pacific and Indian Oceans, PDW and IDW should also have also outcropped north of the ACC and been the source of the shallow waters SAMW and AAIW, as occurs in those basins today.

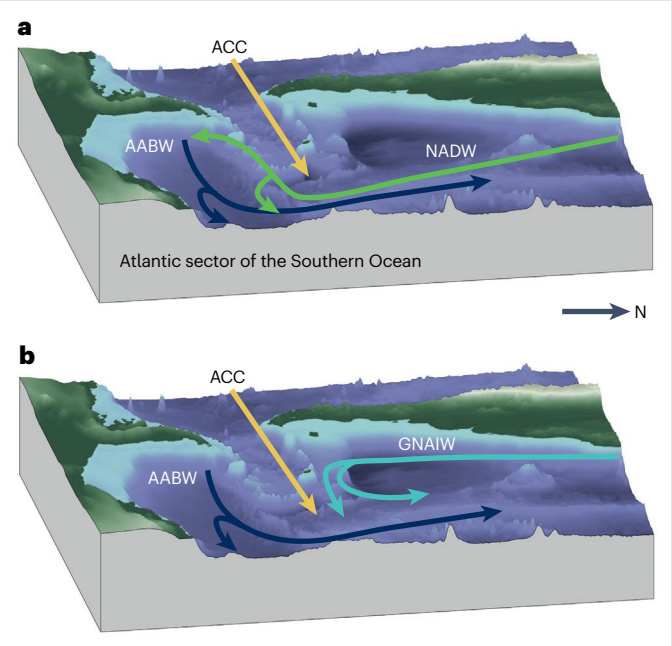

The upwelling of nutrient and DIC-rich deep waters to the surface of the Southern Ocean means that DIC release is partially compensated by the biological uptake of CO_2 during photosynthesis (primarily in the spring and summer). North of the Antarctic Polar Front, in the Subantarctic zone (SAZ), low concentrations of Si limit diatom growth, whereas in the Antarctic zone (AZ), south of the Antarctic Polar Front, diatom growth is limited by Fe[54] and light[55–58]. Thus, the Southern Ocean is an important high-nutrient low-chlorophyll zone in which nutrient consumption is often incomplete, resulting in a high residual, or preformed, nutrient content being advected to depth in AABW, AAIW and SAMW. The organic biological pump represents the sum of the processes that cause the consumption of surface nutrients and sequestration of CO_2 at depth through the production, export and subsurface remineralization of photosynthetic organic matter. In the Southern Ocean, the biological pump is accordingly inefficient, with only about half of the upwelled nitrate used by phytoplankton. The extent of this inefficiency determines the export of excess nutrients into intermediate waters of the upper limb of thermohaline circulation[59] and their subsequent redistribution to most of the low-latitude Southern Hemisphere today[38–40,60] (Fig. 1). This nutrient leakage to sub-thermocline waters helps to sustain global productivity[55,61].

Southern Ocean dynamics during the LGM

During the LGM (~23-18 ka)[62], the climate state of the Earth was fundamentally different from that of the Holocene (10 ka to present). Global temperatures were ~3–6 °C lower than pre-industrial[23,27,63]. Winter sea ice covered the northern portions of the North Atlantic[64,65], moving the locus of deep-water formation southward[66–69]. This altered the formation of NADW, reducing its density and causing the formation of Glacial North Atlantic Intermediate Water (GNAIW)[66,67,70].

Deep circulation changes during the LGM

The Atlantic appears to have had a profound change in overturning circulation during the last glaciation. Numerous lines of evidence indicate both a shoaled geochemical divide in the LGM and a stronger chemical gradient across that divide in the Atlantic. The $\delta^{13}C$ in the tests (shells) of benthic foraminifera is frequently used as a tracer for increased respired DIC in the deep ocean. Compilations of LGM $\delta^{13}C$ from the Atlantic Ocean indicate that the $\delta^{13}C$ enrichment associated with NADW shoaled by about 1,500 m from being centred at ~3,000 m today to being centred at 1,500 m in the LGM[66,67,70], resulting in an increase in southern-sourced waters in the deep Atlantic[68,71] (Fig. 3). $^{231}Pa/^{230}Th$ data demonstrate that the Atlantic MOC) was both shallower[72,73] and potentially more sluggish than today[74]. This shoaled GNAIW was underlain by an expanded, more ^{13}C-depleted water mass[70,71] that from 1,500 to 3,000 m had a North Atlantic sourced component[75]. Evidence from Cd/Ca, a proxy for the nutrient content of waters (Cd_w; which co-varies with nutrient concentrations), also indicates that a chemical divide at ~2,500 m existed within the Atlantic, with nutrient-rich waters residing below nutrient-poor GNAIW[4,76–78].

The changes in Atlantic MOC structure brought on by shoaling of NADW to GNAIW described earlier would have affected the makeup of deep Southern Ocean waters that have a substantial NADW component today[79–82]. GNAIW appears to have sat shallower than the Drake Passage sill depth (~2,500 m)[70,71]. If waters of North Atlantic origin were limited to above ~2,500 m in the glacial Atlantic, then, consistent with the physical and fluid dynamics constraints[8,31], GNAIW would have been largely restricted from the Southern Ocean[19] — a situation corroborated by some models[83] (Box 1). A marked decrease in northern-sourced water in the Southern Ocean was first documented starting in the 1980s[79–82]. An important consequence of the lack of a North Atlantic input, is that PDW and IDW would have become a dominant source for the lower limb (Lower CDW and AABW) of circulation in the Pacific and Indian basins[19,26,84].

Supporting evidence for the lack of deep northern-sourced water in the Southern Ocean and Indo-Pacific during the LGM comes from ε_{Nd}[85,86]. ε_{Nd} has been important for distinguishing past deep-water sources from respired DIC levels (despite some uncertainty in end-member ε_{Nd} and [Nd] that somewhat obfuscate changes in circulation[72–74,87–94]). ε_{Nd} from the Southwest Pacific[85,95], Indian[86] and Southern Oceans[96,97] indicates widespread invasion of Pacific-sourced water at all depths in the LGM[98]. Although some ε_{Nd} studies have suggested the presence of North Atlantic sourced waters in the deep Atlantic in the LGM[99], re-analysis of these data with models appears equivocal[100] and depth transects suggest the presence of Pacific-sourced waters below ~3,000 m[101]. Coupled seawater ε_{Nd}–carbonate ion concentration ($[CO_3^{2-}]$) reconstructions in the South Atlantic[84,102] indicate that DIC-rich water expanded into the deep Southwest Atlantic from the Pacific[103], supporting the interpretation that Pacific waters became the main deep-water source below 3,000 m during the LGM[84,104,105].

In addition to changes in deep-water sources in the several Southern Ocean basins in the LGM, the vertical structure of the water column was altered[19,106]. Compilations of cores that create depth transects of deep-water chemistry[82,107,108] show that the ventilation and sources in the Atlantic did not match the Pacific[19,26,85]. $\delta^{13}C$ and $[CO_3^{2-}]$ in the Pacific

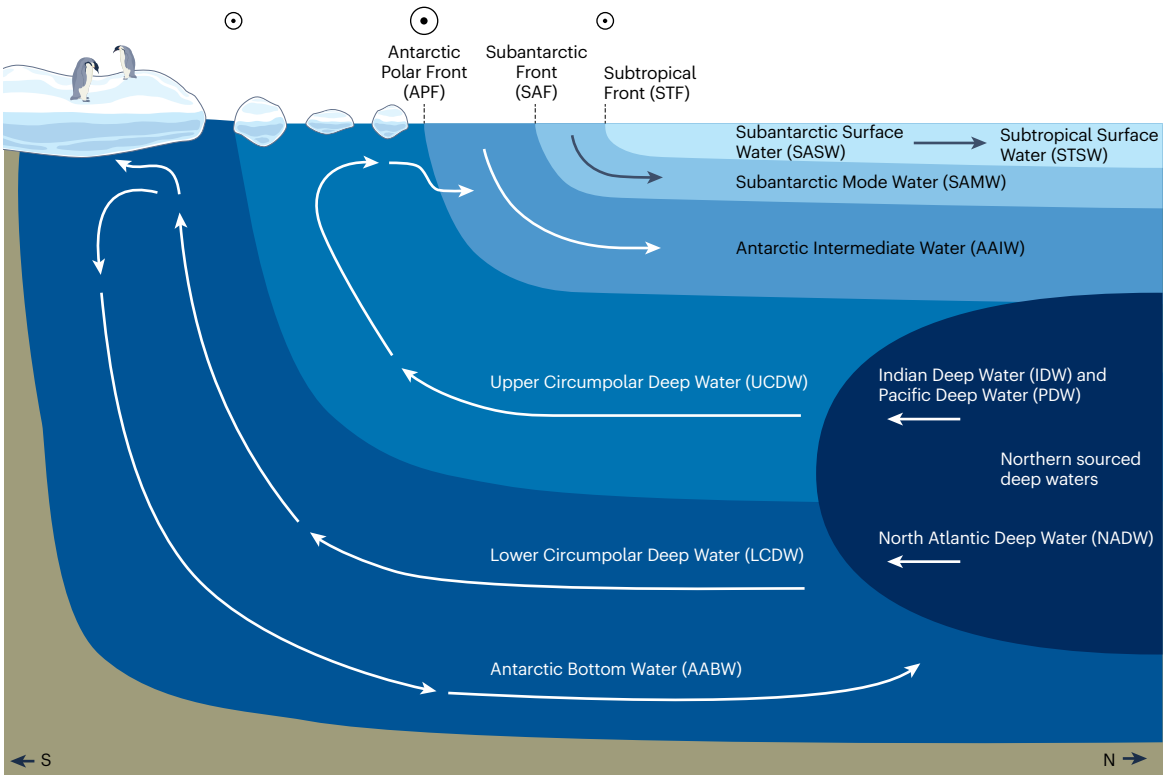

Fig. 2 | Southern Ocean overturning circulation. Arrowheads (circle with dot) depict the net direction of the wind-driven overturning circulation, with size of the arrowhead representing the relative magnitude. Blue shading and flow arrows show water mass formation in the Southern Ocean. The upwelling of deep waters provides nutrients to the surface of the Southern Ocean and brings dissolved inorganic carbon up to exchange with the atmosphere.

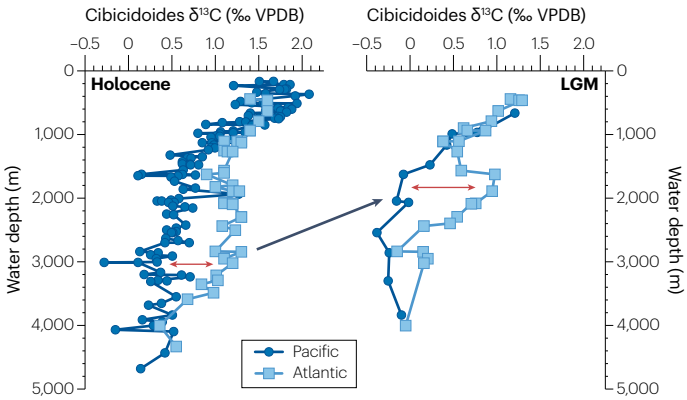

Fig. 3 | Vertical profiles of sedimentary $\delta^{13}C$ in the Atlantic and Pacific. Left, Holocene. Right, Last Glacial Maximum (LGM). Red arrow indicates the depth of the profile minimum in the Atlantic for both times. Note that the minimum is at ~3,000 m in the Holocene, and shallower, at 1,500 m, in the LGM. Data from ref. 270. During the LGM, North Atlantic Deep Waters shoaled to intermediate depths. $\delta^{13}C$ is reported relative to the standard Vienna Pee Dee Belemnite (VPDB).

and Indian Oceans show increased stratification between intermediate and deeper waters[106,109,110] and that Lower CDW in these basins had increased respired CO_2 (refs. 82,111–113). Notably, the geochemical divide in the Indian[114,115] and Pacific basins shoaled by at least ~500 m to above 1,000 m[109,110] (Fig. 3). This shoaled geochemical divide was nearly a kilometre shallower than in the Atlantic[71,85], where intermediate depths had lower respired DIC[116]. Additionally, models show a shoaled divide in the Pacific resulting from the changed global MOC[83] that in turn could have affected shallow water mass formation and wind-driven dynamic pathways related to regional topography[35,44], especially in the Indian Ocean[44]. Taken together, these lines of evidence lend further support to the Drake gateway hypothesis (Box 1).

Lower atmospheric CO_2 in the LGM has been widely attributed to greater sequestration of CO_2 in the deep ocean[22], although storage in the deep Southern Ocean appears to have been significant. Radiocarbon ($\Delta^{14}C$) documents how long DIC been sequestered from the atmosphere. Data from the Southern Ocean[20,117,118] and the Pacific[119–122] point strongly to enhanced carbon sequestration at depths filled by southern-sourced waters, a result that is supported by models[123–125]. The vertical structure of glacial $\Delta^{14}C$ shows that where sequestered carbon resided varied noticeably between basins[126]. Older waters were found below 2 km in the Atlantic[127–129], whereas in the South[119,130] and equatorial[131–133] Pacific, oldest waters were at mid-depths (2–3 km)[119]. Data are more limited but indications are that the Indian Ocean was similar to the Pacific[134–136].

In line with other proxies, $\Delta^{14}C$ shows a shoaled geochemical divide with SAMW remaining well ventilated[109,137,138] and AAIW $\Delta^{14}C$ much lower than today, but relatively much more ventilated than deep water[120]. Overall $\Delta^{14}C$ evidence confines the enhanced glacial respired carbon reservoir to deeper waters[139–142] and, in agreement with $\delta^{13}C$ reconstructions[19], confirms that there was greater DIC storage in the Pacific[120,142] relative to the other basins. The shoaling of the geochemical boundary has been suggested to have contributed to stronger isolation between the upper and lower limbs by reducing deep topographic turbulent mixing[17] and along with increased deep ocean salinity[143] resulted in increased ocean stratification. An associated increase in deep ocean carbonate compensation through enhanced dissolution of deep ocean carbonates, for example[144], would have further aided the sequestration of CO_2. The water mass geometry and mixing changes in the LGM would have increased the standing volume of cold, respired carbon-rich deep waters at the expense of warmer, carbon-depleted waters[84,145]. These carbon-rich waters were likely sourced from the Southern Ocean giving surface processes of air–sea exchange and biological uptake increased influence on the glacial CO_2 ocean–atmosphere balance.

Today, the Southern Ocean is a high-nutrient low-chlorophyll zone in which key limiting micronutrients prevent phytoplankton from fully using the available nutrients, resulting in a inefficient biological pump. Thus, the potential exists for the Southern Ocean biological pump to drawdown more CO_2 in the past through either an increase in the supply of nutrients or the alleviation of limitations on production by iron availability allowing a greater proportion of the nutrients to be consumed by phytoplankton. The ecological differences between the carbonate-dominated SAZ and the silica-dominated Polar Frontal Zone and AZ affect the interplay of micronutrients on productivity producing spatially distinct biopump regimes[146]. During the LGM, an increased flux of Fe-bearing dust to regions of the Southern Ocean that are today Fe-limited facilitated biophysical changes to the biological pump[147]. Specifically, both biogenic sediment accumulation rates and $\delta^{15}N$ and $\delta^{13}C$ values were higher in the SAZ, indicating enhanced export production[148] and surface nutrient consumption[53,149,150] that likely reflected enhanced iron availability[148,149,151,152], which subsequently enhanced CO_2 sequestration in the deep ocean during the later stages of the last glaciation[59,153]. Despite purported increases in iron availability, export production decreased in the AZ[29,154–157]. This decrease co-occurred with an increase in relative nutrient consumption, suggesting that nutrient supply decreased more than nutrient demand and implicating reduced upwelling of nutrient-rich deep waters in the AZ[152,158–162]. Reduced AZ nutrient supply and increased nutrient demand in the SAZ likely worked together drawing CO_2 down leading into glacial periods[15,153,163].

Enhanced export production from the surface paired with the consequent respiration of that organic matter at depth[164–166] resulted in not only the accumulation of respired carbon but also the depletion of oxygen in deep waters. More intense oxygen consumption at depth can also be the result of prolonged residence in the abyss[124]. Widespread lower oxygen concentrations in southern-sourced waters throughout the Pacific have been documented by qualitative (for example, redox-sensitive trace elements; Cd, Mo, U and foraminiferal assemblages) and semi-quantitative proxies of oxygenation including biomarker preservation[167,168] and the foraminiferal estimated bottom-water to anoxic pore-water $\delta^{13}C$ gradient ($\Delta\delta^{13}C_{epifaunal\text{-}deep\ infaunal}$)[169,170]. These proxies suggest deep-water oxygen concentrations as low as ~35 μmol kg^{-1} in the equatorial Pacific[167,169,171,172]. If oxygen-depleted southern-sourced waters filled roughly half of the volume of the LGM oceans, and assuming the deficit stems from respiration rather than disequilibrium, an additional ~850 PgC could have been stored in the oceans relative to today[125,167,171,173–175]. The evidence for a decline in deep ocean oxygenation, both in the Southern Ocean[150,164] and beyond, is consistent with an enhanced biological pump[172,176,177] and/or reduced ventilation of AABW or reduced gas exchange via a mechanism such as expanded sea-ice coverage in the Southern Ocean[178].

In summary, multiple lines of evidence have solidified the understanding that LGM changes in ocean circulation went beyond the likely shoaling of NADW to GNAIW in the Atlantic, and the consequences of the loss of a North Atlantic input had implications for water sources and water mass structure in the Southern Ocean. As discussed earlier,

extensive reconstructions of past seawater $\delta^{13}C$ of DIC, $[CO_3^{2-}]$, ε_{Nd}, oxygenation, nutrients and ^{14}C have verified that globally, deep waters in the southern basins were southern-sourced, contained more carbon in the form of DIC (that had been sequestered for longer periods than in the Holocene) and that these same deep waters had lower oxygen levels. These Atlantic–Pacific differences, in addition to differences in the depths of their respective chemical divides, support the concept that there was a diminished northern influence in the deep southern basins[19,85], leading to the hypotheses of an enhanced role of Southern Ocean dynamics in global carbon cycling.

Glacial Southern Ocean surface dynamics

A number of dynamic changes in the surface Southern Ocean associated with global cooling appear to have served as important amplifiers and/or drivers and are accepted to have enhanced sequestration of CO_2 in the ocean, independent of changes in overturning circulation. Movement of fronts would have modified the dynamics of the ACC and its eddy field[35] affecting transport of mass and heat poleward as well as the closure of the overturning circulation. Enhanced nutrient utilization would have improved the efficiency of the biological pump, contributing to the drawdown of CO_2 (refs. 179–187). Advances in the understanding of degassing mechanisms and locations in the Southern Ocean[188] imply that these LGM physical changes could have combined to depress degassing[2,17,189].

Globally, quantitative SST estimates have demonstrated that the surface ocean was colder during the last glaciation[190,191]. Overall, reconstructions[185] suggest that the Southern Ocean was ~4 °C cooler than the Holocene[192–195]. The picture of overall cooling can be improved by using multiproxy SST records[180,192,196] that are based on different plankton species with demonstrated different seasons of growth today[197] that can be used to reconstruct seasonal differences in the past. Multiproxy SST records are available from the Australia–New Zealand region that show that although summers were colder by ~4 °C, winters were 4–7 °C cooler[180,192,196]. This analysis allows us to infer that although summers were colder by about the same as global averages, winter SST in subpolar waters to the south and east of New Zealand cooled as much as 3 °C more, implying an intensification of winter season cooling[192,193,198].

Reconstructing the past location of fronts relies on using their hallmark, a steep gradient in SST[43]. Consequently, our understanding of the movement of Southern Ocean fronts rests largely on the reconstruction of palaeo SST. The enhanced SST gradients associated with frontal locations indicate northward frontal shifts during the last glaciation[180,192,198] with abundant evidence that Southern Ocean fronts shifted northward in most sectors of the Indian[199–201] and Pacific basins[198,202,203]. This movement was restricted only where land masses constrain their movement, such as east of New Zealand[192,196,198] and south of Tasmania[180,204]. The largely unrestricted movement of the Subtropical Front northward to the south of Africa[182,199,205], across the Indian Ocean, and south of Australia[200,202] was as much as 8° of latitude (Fig. 4). Frontal movement also likely contributed to the enhanced cooling observed adjacent to frontal locations in the past[180,192,193,198].

Today, a fundamental feature of the climate system in the Southern Hemisphere is the alignment of the Southern Westerly Winds with Southern Ocean fronts. Wind stress largely determines the frontal locations along with bathymetric steering[42,206] and landmass placement[207]. The position of the wind belt, SST gradients and their associated fronts vary latitudinally on a seasonal basis, being more equatorward in the austral winter and more poleward in the austral summer, especially where they are free to move[42,43]. We use these seasonal shifts as an analogy for LGM northward frontal movement (Fig. 4). The position of the fronts in the past, combined with terrestrial records of atmospheric temperature, are a potential indicator for past Westerlies placement. During the LGM, the mid-latitude cooling seen in proxy reconstructions has frequently been attributed to meridional shifts in the Southern Westerlies, resulting in changed weather patterns[203,208,209]. Marine and terrestrial climate data have also been interpreted as an increased high-latitude influence along the northern rim of the Southern Ocean, characterized by a more persistent northerly position of the Southern Westerlies in the LGM[208–210] and through the early deglaciation[196,203,211].

Northward frontal movement in the LGM[180–182] and the expansion of sea ice around Antarctica are well documented[183–187]. These shifts would have induced shoaling in the upper limb of the overturning circulation[17], a phenomenon well documented in depth transect studies that document the depth extent of water masses[85,109] (Fig. 2). The current understanding of degassing mechanisms and locations in the Southern Ocean[188] indicates that wind shifts away from optimal degassing configurations could have enhanced CO_2 sequestration[2,189] in conjunction with increased nutrient utilization.

Simulations of the Southern Ocean using box models and intermediate complexity models tend to simulate increased oceanic carbon uptake with increasing winds[1–3,32,189,212–215], whereas complex ocean general circulation models tend to simulate enhanced outgassing without a consistent sign in CO_2 response to meridional shifts in Southern Westerlies[214,216,217]. This variability among model types illustrates the complexity of ocean-carbon cycle dynamics while raising the awareness that some of the widely used, simplified 2D conceptual reconstructions can often be misleading on finer scales[35]. However, model intercomparisons are showing improved performance and more realistic patterns in wind stress forcing[216], and model-data comparisons illustrate predicable linkages among temperature, wind and meltwater[217]. Models do agree that an increase in the strength of SHW leads to enhanced outgassing and vice versa[214]. Taken together, sea-ice and wind changes likely contributed to the physical stratification and isolation of the glacial deep ocean, enhancing its ability to hold more CO_2. To the extent that deep stratification and isolation is an essential feature of glaciation[143], these conditions set the stage for Southern Ocean dynamics to have a role in the deglaciation[7,18,19,28].

In summary, many factors contributed to lower atmospheric CO_2 in the last glaciation, and changes in overturning circulation appear to have greatly altered the sources and structure of waters in the Southern Ocean across basins[19,85]. Increased ocean stratification and reduced nutrient supply to the surface[16,158,218] likely decreased the efficiency of the biological pump. Decreases in temperature and dynamic northward movement in frontal locations can be linked to reduced southward transport supported by eddy mixing[50] and diminished air–sea exchange of CO_2, contributing to carbon-rich deep waters and deep carbon sequestration. Hence, global glaciation conditions were likely amplified by dynamics in the Southern Ocean.

Southern Ocean influences on deglaciation

We now shift focus to discuss the events of the first half of the last deglaciation. Temporally, we focus on HS1 (14.5–17.5 ka) and the ACR (12.9–14.5 ka), because later deglacial events have very muted expression in the Southern Ocean. We review the Southern Hemisphere dynamics that were influenced by the initial atmosphere–ocean warming during the last deglaciation, including the movement of fronts and the timing of the release of carbon sequestered during the LGM.

Global onset of deglaciation

Extensive evidence compiled since the 1970s has demonstrated that the last glacial termination proceeded in multiple steps (Box 2). Early work in the 1980s identified that the warming during the deglaciation (or last termination) was punctuated by a brief period of rapid return to cold, glacial-like conditions followed by abrupt warming, with these two warming periods previously referred to as termination 1a and 1b[219]. Further work centred on the North Atlantic inferred that there was an intense Northern Hemisphere cooling that followed the first deglacial warming and punctuated the two warming pulses, dubbed the Younger-Dryas (YD; 12.8–11.7 kyr)[220]. The YD was initially conflated with the ACR (12.9–14.5 ka), giving the appearance of a synchronous two-step deglaciation globally. This confusion was likely exacerbated by the fact that climate records from different substrates such as ice cores and carbonates are necessarily based on various stratigraphic and chronologic tools. Each has inherent uncertainties that put practical limits on precise age control. Cross-calibrating different proxy records to ensure the best possible common stratigraphy is important for good chronology and essential for determining leads and lags between individual proxy records. For example, differences among Antarctic and Greenland ice core records have been reconciled using methane levels trapped in the ice[221]. Ice core climate records are then cross-calibrated with speleothems using $\delta^{18}O$ (ref. 222), whose primary stratigraphy is based on U-Th dating[222] to ensure that global climate records have a common chronology.

With improved radiocarbon dating tools and calibrations[223] resulting in better age control, it became clear that Southern Hemisphere YD responses are frequently absent[224] and that the two-step deglaciation signal varied regionally in both magnitude and direction[23]. Observed warming in the Southern Hemisphere thought to coincide with cooling in the Northern Hemisphere during the deglaciation has been linked to changes in meridional oceanic heat transport[225]. The consistent interhemispheric temperature differences[226] were dubbed the bipolar seesaw[3,225–227]. Although widely used, the term bipolar seesaw does not accurately represent the interhemispheric deglacial heat transport dynamics, as the timing of temperature changes and the interplay of forcing factors throughout the deglaciation taken together now appear more complex[23,50,228]. Nonetheless, focusing on the interhemispheric signals can help clarify the link between warming[23,196,224], ocean circulation changes and the deglacial increase in atmospheric CO_2 (refs. 22,181,229).

In current understanding, the onset of deglaciation is synchronous with the start of HS1 (~18 ka) and the rise in atmospheric CO_2 (ref. 23) (Box 2). The widespread synchronicity of HS1 events in the North Atlantic region has been characterized as having fully antiphased temperature responses between the hemispheres. However, HS1 is more fully described as pervasive wintertime cooling and summertime warming in the Northern Hemisphere[230,231] with sea-ice-intensified wintertime cooling in the North Atlantic region appearing to have masked summertime warming[228], which has been largely summed up as cooling in many records[22,23].

Southern Hemisphere early warming

It appears that early warming in the Southern Hemisphere[23] preceded the global shifts occurring at 18 ka[22,184,232], hinting that processes in the south could have tipped the balance towards deglaciation[233]. Southern

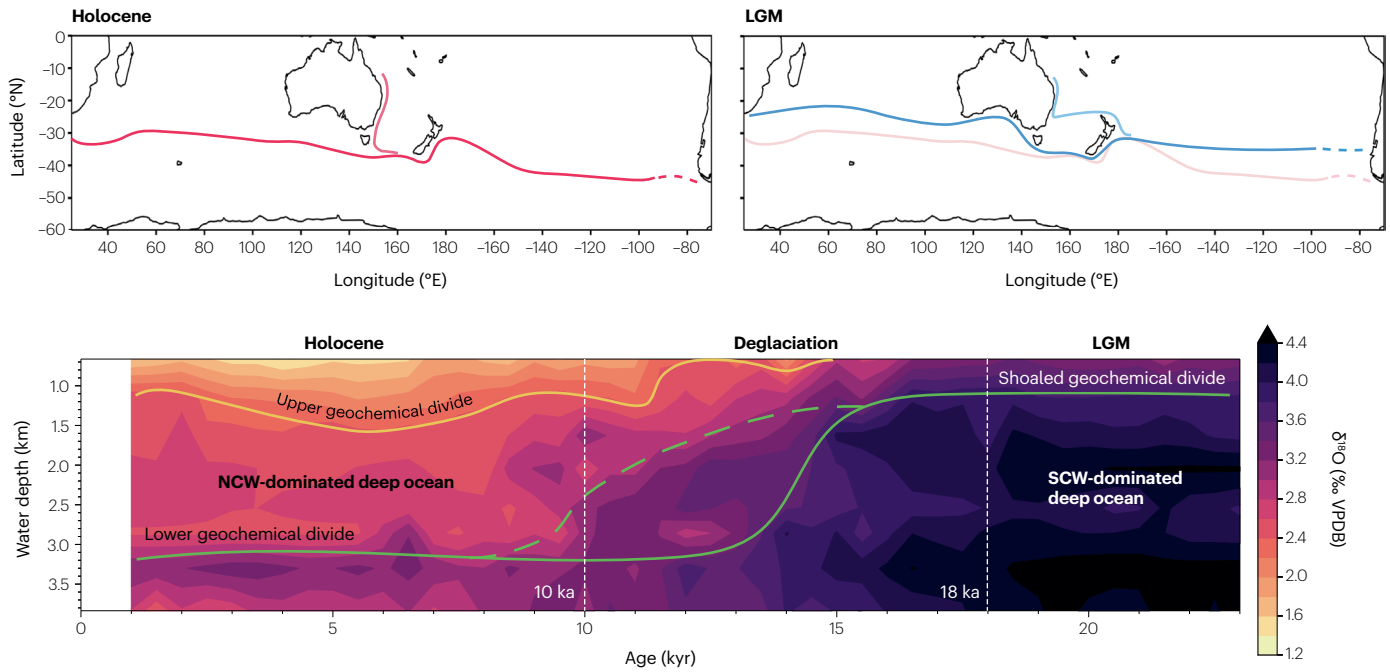

Fig. 4 | Surface front and deep geochemical divide variations from Glacial-to-Holocene conditions. Maps show placement of the Subtropical Front in the Holocene and estimated positions in the Last Glacial Maximum (LGM), with the suggested position of the East Australian Current in the Holocene (dark pink line, top left panel) and its displacement in the LGM (blue line, top right panel), referred to as the Zealandia Switch[7]. The vertical section (lower panel) shows changes in the deep geochemical divide structure in a vertical $\delta^{18}O$ transect through time for the Southwest Pacific. Breakdown of the intensified geochemical divide and ventilation occurred early in the deglaciation, preceding the reintroduction of northern-sourced waters to the Southern Ocean. The presence of Northern Component Water (NCW) between ~2 and ~3 km in the Holocene is supplanted by Southern Component Water (SCW) in the LGM.

Box 2

Southern Hemisphere deglacial events and their role in deglacial climate change

The last deglaciation proceeded in multiple steps also called millennial-scale climate events. The names, timing and extent of these events can be confusing as the chronology and extent are the subject of ongoing research.

Henrich layers and events

Deposits of iceberg rafted, detrital material have been identified in the North Atlantic, and found to coincide with massive meltwater discharge during glacial periods, collectively termed Heinrich Events[272]. These events were subsequently linked to cold intervals in temperature records from the North Atlantic region[273], named Heinrich Stadials. The most recent of these, Heinrich Stadial 1 (HS1), occurred at the start of the last deglaciation, originally dated as 14.6–18 ka[274] but more recently defined as (HS1: 14.5–17.5 ka), which can be subdivided into two intervals of cooling, HS 1.1 and 1.2 in high-resolution stratigraphic studies[275].

The start of HS1 has become synonymous with the onset of deglaciation, which is a widely recognized and strongly synchronized signal in the Northern Hemisphere. The beginning of HS1 coincided with the rise in ocean $\delta^{18}O$ signalling the onset of boreal continental ice sheet melting (see the figure, part **d**) that resulted in a flood of meltwater to the North Atlantic, recorded by the presence of ice-rafted debris, the hallmark of Heinrich Events. The substantial input of fresh water to the North Atlantic resulted in a glacial meltwater cap credited with the shutdown of Atlantic thermohaline overturning circulation (see the figure, part **c**)[73,276]. This chain of events both cooled the Northern Hemisphere and altered the hydrological cycle of interannual and interdecadal events such as the East Asian monsoon (see the figure, part **b**)[277]. Globally, HS1 is also notable for the rapid drop in atmospheric $\Delta^{14}C$ (ref. 278) (see the figure, part **a**)[279] that mirrors the atmospheric increase in CO_2 (see the figure, part **e**).

There is a notable alternation in temperatures between the hemispheres during HS1 that has been attributed to a synergistic interplay between the weakened thermohaline overturning circulation and cooling in the north driving a southward shift of the Intertropical Convergence Zone and the southern Westerly wind belt[3,280], suggesting a fundamentally Northern Hemisphere heat transport influenced system[241]. The different timings of events observed in the Southern Hemisphere suggest independent influences and/or amplifications. Recent work has suggested that the influence of the latitudinal variations in orbitally driven insolation could have been a factor (see the figure, part **f**)[28,159] causing early Southern Hemisphere warming as a substantial driver[28]. This possibility is supported by timing offsets in models between notable Southern Ocean events and Northern Hemisphere thermohaline changes with the interpretation that the Southern Hemisphere and Southern Ocean are a dynamic coupled system with multiple equilibrium states[21,280].

Antarctic Cold Reversal (ACR; 12.9–14.5 ka)

A cooling largely confined to mid and higher Southern Hemisphere latitudes. The ACR cooling was first identified in Antarctic ice cores

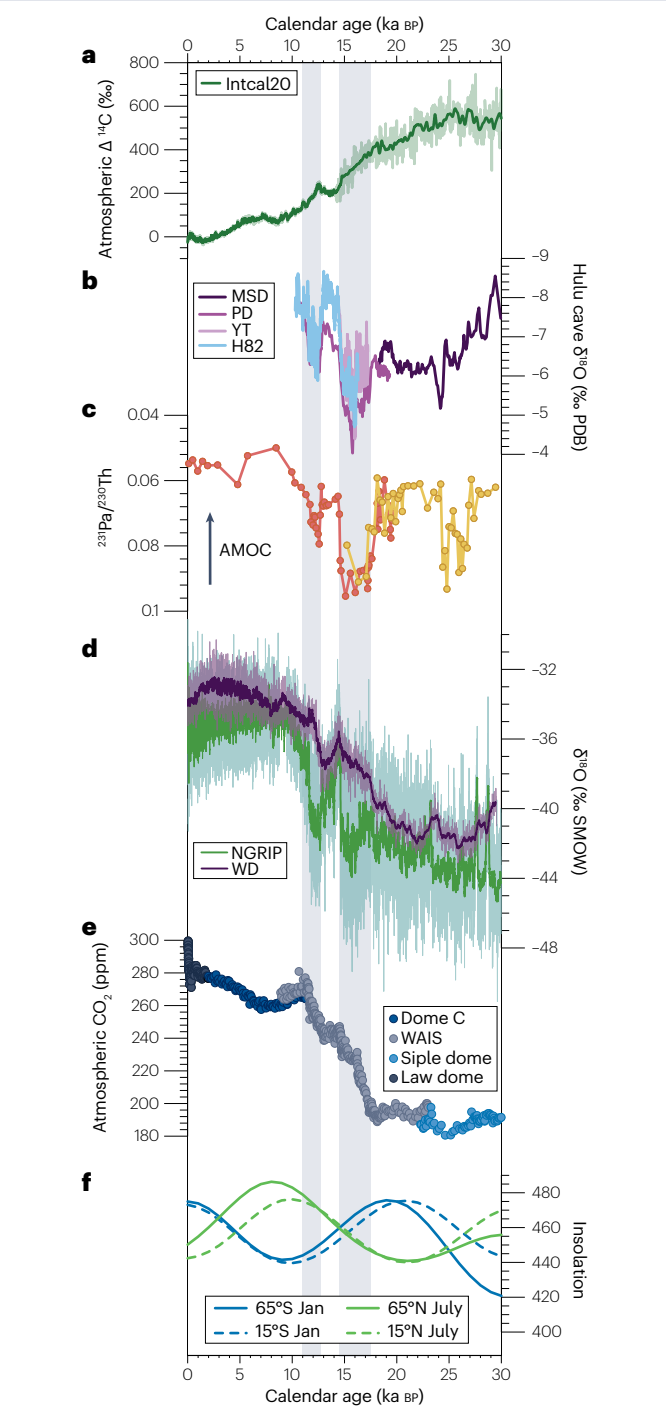

(continued from previous page)
(see the figure, part **d**), and is also observed in mid-to-high latitude marine and terrestrial temperature records across the Southern Hemisphere. Precise dating has now established that it precedes Northern Hemisphere cooling during the Younger-Dryas and that it is instead coeval with Bølling–Allerød (BA)[22,23,281],a warm interval confined to mid- and high-Northern Hemisphere latitudes (14.5–13 ka) (ref. 220). As such, this is the embodiment of the bipolar alternation in temperature signal (see the figure, part **d**). The rapid Northern Hemisphere warming in the BA has been attributed to the restart of thermohaline circulation after the HS1 pause (see the figure, part **c**). The contrasting cooling of the ACR has been attributed to re-expansion of sea ice in the Southern Ocean as summer insolation in the Southern Hemisphere dropped. These Southern Hemisphere factors have been linked to shifting Westerlies that reduced upwelling[29] and likely caused the pause in the global rise in CO_2. The weak influence, or the lack of Atlantic Meridional Overturning Circulation influence on Southern Ocean processes during the ACR, could reflect the fact that northern-sourced waters were still shoaled at that time[73] or might reflect multiple changes in Southern Ocean dynamics, including warming of the deep ocean[27] that dampened the response as the Earth had substantially exited the glacial mode[50].

Younger-Dryas (YD; 12.8–11.7 ka)
A rapid return to near-glacial conditions largely confined to the Northern Hemisphere. The YD, initially observed as a rapid cooling event centred on the North Atlantic, appears to be restricted to the Northern Hemisphere (see the figure, part **d**). The intense YD cooling in Greenland is attributed to a reduction in thermohaline circulation, which was substantial but smaller than in HS1 (ref. 72) (see the figure, part **c**). Nonetheless, the impact on Northern Hemisphere temperatures and hydroclimate as far away as Asia was enormous (see the figure, part **b**)[23,222]. The YD was concurrent with the resumption of Southern Ocean upwelling and reinvigoration of the atmospheric CO_2 increase (see the figure, part **e**)[29]. The bipolar influence during the YD appears to have been weaker than the ACR during which many Southern Hemisphere temperature records show little or ambiguous responses[23,196,209,224], rather than the opposite response as observed in the ACR. Likewise, this lack of Southern Hemisphere response could have been because northern-sourced waters remained shoaled[73] and therefore still restricted from the Southern Ocean[19]. Alternatively, the insolation gradient between the hemispheres had widened (see the figure, part **f**).

Holocene (11.7 ka to present)
The onset of the warm Holocene period marks the termination of the transition out of the last glacial period at about 11.7 ka.

Abbreviations in this figure: IntCal is the intercalibration of ^{14}C project (**a**); MSD, PD, YT and H82 are individual speloethem names (**b**); Atlantic Meridional Overturning Circulation (AMOC) (**c**); North Greenland Ice Core Project (NGRIP)[282], West Antarctic Divide (WD) ice cores (**d**); Dome C, Siple dome and Law dome are ice cores from the West Antarctic Ice Sheet (WAIS)[283,22] (**e**); $\delta^{18}O$ values are reported to standard mean ocean water (SMOW).

Hemisphere mid-latitudes (~35–45 °S) SST started warming around 21 ka[181,193,234] leading, by about 3 ka, both the northern expression of HS1 and warming in Subantarctic waters[180,196] (Fig. 5). Furthermore, seasonal SST analyses suggest mid-latitude winters warmed before summers and warmed faster[196,235] intensifying the warming effect. In the Australia–New Zealand region, these mid-latitude seasonal differences have been attributed to changing Southern Westerlies influences across the seasons during the deglaciation[196,208–211]. Farther south, in Subantarctic regions, summer warming began later, between ~18 and 19 ka[180,236,237]. Antarctica warmed nearly synchronously with the CO_2 rise[238,239], and warming of waters south of the SAF matched that of the Antarctic continent[135,237]. Present-day Southern Ocean dynamics dictate that the eddy field across the ACC would have transported this subtropical heat poleward to the upper layers of the Southern Ocean[35].

Early mid-latitude warming in the Southern Hemisphere corresponds to insolation increases at these latitudes around 21 ka (Fig. 5a and Box 2) with insolation-driven lengthening of summers in Southern Ocean latitudes[233] that has been hypothesized as one mechanism for the Southern Hemisphere leading or having a role in driving the deglaciation[28,159,240] (Fig. 5a and Box 2). The early, rapid loss of sea ice in the Southern Ocean at about ~20 ka[184] coincided with maximum summer (January) insolation at 65° S[28] (Fig. 5) with initial pulses of deep ocean warming accelerating at ~18 ka[27]. Although the start of HS1 coincides with the initiation of the global rise in atmospheric CO_2, it is notable that, similar to bottom water temperature, CO_2 did not decline and sea ice did not fully rebound again after HS1 — distinguishing it from a typical abrupt Heinrich bipolar climate event[241–243] (Box 2). Notably, more than half of the warming in the mean global ocean temperature[27] and half the CO_2 increase occurred across HS1 and before the Northern Hemisphere Bølling–Allerød warming event when there was the first reinvigoration of, but not deepening, Atlantic MOC[19,73] (Box 2). The southern lead in these events suggests Southern Hemisphere processes influenced deglacial initiation[27,50]. Critically, the rise of CO_2 above a threshold level of 230 ppm has been suggested to lock the planet into an interglacial mode as long as CO_2 remains above that level, lagged Southern Hemisphere warming, so CO_2 could not have driven that warming[2].

The influence of shifting fronts on CO_2 release

Early warming beginning around 21 ka in the subtropical Pacific around the North Island of New Zealand[196] led the SST warming in Subantarctic waters around the South Island of New Zealand and Tasmania[180,196,198]. By contrast, SST warming in Subantarctic waters was notably synchronous with New Zealand glacial retreat at ~18 ka[7]. These latter events do correspond to a step-change in the surface water source and the thermocline thickness to the north of New Zealand that indicates a shift in cross-Tasman flow[244]. This evidence for circulation changes lends some empirical support to the 'Zealandia Switch' hypothesis that links glacial retreat on the New Zealand subcontinent to a hypothetical shift in cross-Tasman flow at ~18 ka[7] (Fig. 4). The Zealandia Switch hypothesizes that the northerly migration of the Westerlies in the LGM caused a fundamental shift to a restricted South Pacific subtropical gyre system owing to the land mass placement in the region (Fig. 4), an assertion supported by model simulations that provides a mechanism for the

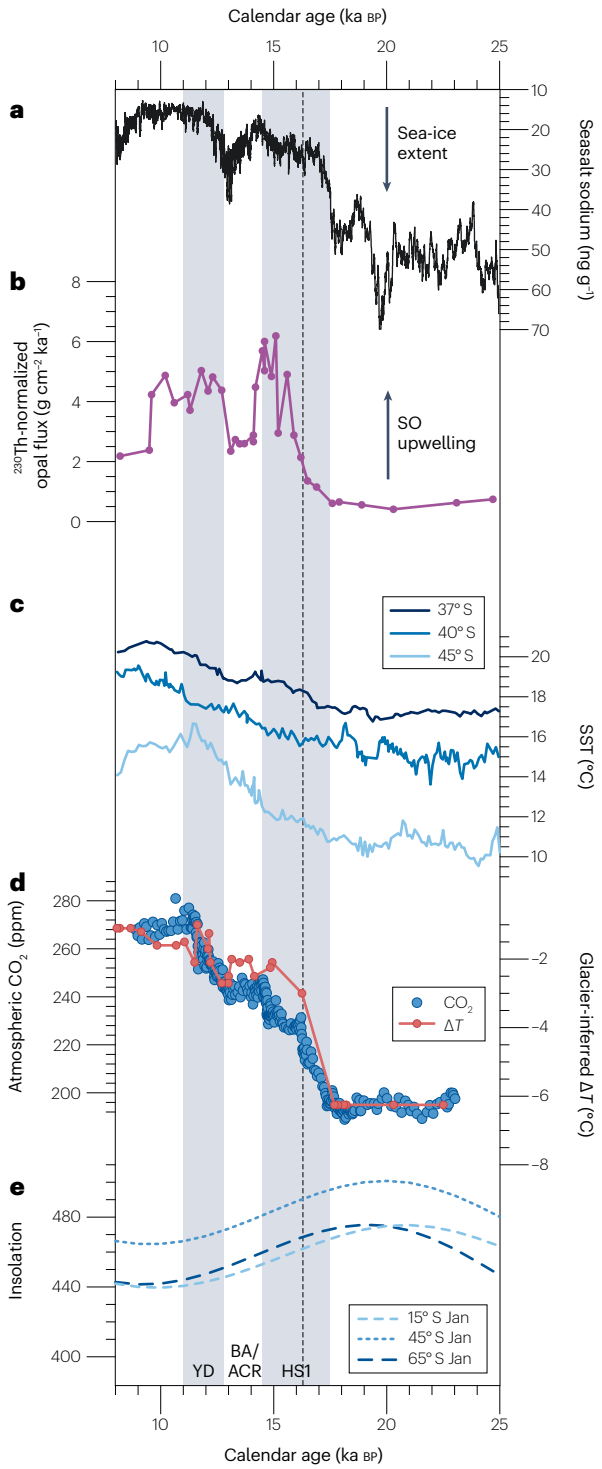

Fig. 5 | Deglacial time series. a, Seasalt sodium in ice cores (a sea-ice extent proxy)[184]. **b**, Southern Ocean (SO) upwelling, as indicated by opal accumulation[29]. **c**, Alkenone-based sea surface temperature (SST) reconstructions from the east of New Zealand[196] interpreted as summer SST. **d**, Mean ocean temperature[27], atmospheric CO_2 (ref. 22) and relative temperature change[27]. **e**, Total solar insolation for the months and latitudes indicated. The time intervals are displayed on the *x*-axis, which include: ACR, Antarctic Cold Reversal; BA, Bølling–Allerød; HS1, Heinrich Stadial 1 and YD, Younger Dryas. Southern Ocean upwelling increased and sea-ice extent decreased before the main onset of deglaciation, CO_2 release and warming.

southern origin for the dominant phase of the last glacial termination[7]. Integral to this mechanism is that mid-latitude warming was the result of southerly migration of the Westerlies that in turn caused an abrupt reorganization at ~18 ka that expanded the subtropical gyre system reinitiating the modern configuration characterized by a strong East Australia Current and dominant cross-Tasman flow from Tasmania to the South Island of New Zealand[7] (Fig. 4).

Evidence for the importance of Southern Ocean dynamics and Southern Hemisphere conditions on the early deglaciation that eclipsed the influence of MOC circulation is solidified by ε_{Nd} data. All deglacial time series of ε_{Nd} in the southern Atlantic[84], Indian[86,97,105] and SW Pacific[245] indicate that the reintroduction of Atlantic-sourced waters into the Southern Ocean did not occur until after Atlantic MOC recovered, possibly in the Bølling–Allerød and more likely during the YD[73]. This interpretation holds even when potential changes in the end-member ε_{Nd} of Atlantic-sourced waters are taken into account[246]. The individual timing varies, but a shift in ε_{Nd} is generally seen around the time of the ACR or after[84,86,247]. Evidence from the Atlantic suggests that it was not until after the YD that Atlantic MOC deepened enough[73] to re-enter the Southern Ocean[19,86] (Box 1). It is noteworthy that NADW reinvigoration lagged substantially in the early warming of the mean ocean[27], indicating that AABW warmed before there was NADW input[242,248,249], again suggesting a southern driver in the deglacial initiation.

Flushing of respired CO_2 from the deep ocean across the deglaciation is well documented. Time series of $\Delta^{14}C$[120,121,125] and carbonate ion concentration ($[CO_3^{2-}]$) determined using B/Ca (ref. 113) along with $\delta^{13}C$ (refs. 26,109) in the South Pacific all indicate that the deep South Pacific lost a substantial portion of the glacially sequestered DIC across HS1. The deep Pacific was flushed of low $\Delta^{14}C$ (refs. 120,125), whereas intermediate depth records of ^{14}C were more variable, which could have been a consequence of dynamic changes in water mass geometry. High-latitude Southern Hemisphere records[117,138,140–142,250] have so far found little evidence of $\Delta^{14}C$-depleted waters at intermediate water depths in the deglaciation. This absence contrasts with pulses of $\Delta^{14}C$-depleted waters observed in Northern Hemisphere locations that have been suggested to document the path of CO_2 release at low latitudes[251–255] purportedly from the Southern Ocean (although the significance of equatorial degassing has been disputed[256]). Deglacial records of surface ocean pCO_2 based on boron isotopes have documented CO_2 release to the atmosphere from the equatorial Pacific and Southern Ocean[194,257–260], suggesting a shallow water tunnel connection between them. Although the resolution and variation between equatorial and Southern Ocean locations leaves the timing somewhat unclear, at a minimum, the Southern Ocean appears to have been an important site of CO_2 release across the deglaciation[194,257].

A distinct deglacial pace in the Southern Hemisphere

Although HS1 began at ~18 ka, many notable events in the Southern Hemisphere have been documented midway through HS1 at ~16.3–16.5 ka, suggesting a regional event that influenced CO_2 release. The onset of intense upwelling in the Southern Ocean[29] (Fig. 5b) at ~16.5 ka (Fig. 5, dashed line) coincided closely with evidence for better ventilation of AAIW at ~16.3 ka[109,260] and a widely noted spike in atmospheric

CO_2 increase at ~16.3 ka[22], all attributed to the release of respired CO_2 from the ocean (Fig. 5e). Multiseason SST records with high enough resolution show a decrease in the winter latitudinal temperature gradients centred on 16.3 ka[196] also coincident with a sharp decrease in the atmospheric $\delta^{13}C$ (ref. 24) and $\Delta^{14}C$ of atmospheric CO^2 (ref. 223), again attributed to a combination of the release of respired CO_2 from the ocean and terrestrial biosphere. Collectively, these events suggest that halfway through HS1 (~16.3 ka), Southern Ocean dynamics were involved in releasing a pulse of CO_2 to the atmosphere well before North Atlantic sourced waters re-entered the Southern Ocean[19,86].

The ACR was a cold period that is recognized throughout the Southern Hemisphere, which represented a partial return to glacial conditions. Occurring at the same time as the Northern Hemisphere Bølling–Allerød warming event, it is an interhemispheric temperature seesaw. The ACR was represented by widespread Southern Hemisphere cooling at mid-latitudes in both terrestrial[23,224] and marine[196] records. ACR cooling coincided with expanded sea-ice extent[184] and more northerly frontal positions[180,181]. During the ACR, the CO_2 release paused[22], which indicates that these conditions were not favourable for CO_2 release and could be attributable to diminished upwelling in the Southern Ocean[29]. Reduced shallow ventilation at this time[109] supports the connection between surface dynamics in the Southern Ocean and diminished deep-water degassing. Increased export production and nitrogen isotopic evidence during the ACR for oxygen deficit zone expansion outside the Southern Ocean suggest enhanced nutrient supply to low latitudes via SAMW and decreased nutrient utilization similar to the LGM[177,261,262]. Following the ACR, resumed warming[23,184,196], sea-ice reduction and northward front movement[180] occurred. Notably, there is little or no YD expression in mid-latitudes and lower latitudes of the Southern Hemisphere[224], making the ACR the last notable climatic event in the deglacial Southern Ocean.

Nutrient utilization and CO_2 sequestration

Changes in export production and nutrient utilization during the deglaciation have also been linked to past changes in winds, deep ocean stratification or biological uptake and export that in turn could have changed the balance of the air–sea flux and influenced CO_2 sequestration. With the onset of HS1, dust-borne iron fertilization appears to have waned in the South Atlantic Polar Frontal Zone and AZ[149,153]. In the Atlantic SAZ, export production and nutrient consumption decreased[153] whereas deep ocean oxygenation increased, consistent with the interpretation that productivity was driven by diminished dust supply and iron availability[149,153]. To the south, export production increased abruptly whereas nutrient consumption decreased, consistent with the intensified upwelling in the Polar Frontal Zone[29,160,263]. However, dust fertilization played a lesser role in the Pacific[264]. Similarly, in the AZ of the Indian Ocean, correlation between export production and dust proxies suggests reduced nutrient utilization through the deglaciation[159]; these are smaller changes than observed in the Atlantic[265]. Nutrient utilization in the Indian Ocean SAZ remains unconstrained. The variation among basins and between Southern Ocean zones leaves the influence of nutrient utilization in the earliest deglaciation uncertain.

Notable observations gleaned from focusing on the Southern Ocean during the last deglaciation are as follows. Waters of North Atlantic origin that were largely restricted from the deep Southern Ocean during the LGM (23-18 ka) were not detected until after the ACR (12.9–14.5 ka). The initial accumulation of heat in mid-southern latitudes[50] might have helped prime whole ocean warming in the early deglaciation[27], prompting the interpretation that regional insolation could have been an important driver of the initial deglaciation[28,159,193]. This early warming has led others to suggest drivers in the first half of the deglaciation, which might have been atmospheric[3,50], or driven by Southern Ocean–Atmosphere dynamics[7,19]. Other theories call on Southern Hemisphere total insolation levels forcing deglaciations[233] and others invoke different aspects of Southern Hemisphere orbital parameters as triggers for deglaciations[28,159,240].

Summary and future perspectives

The ocean is the largest reservoir of rapidly exchangeable carbon on the surface of the Earth, which at present contains 45 times more CO_2 than the atmosphere[266]. Variations in atmospheric CO_2 during the last glaciation and deglaciation were likely caused by climate-related changes in ocean dynamics controlling global CO_2 partitioning with the atmosphere[267]. Studies based on proxies found in marine sediment cores have guided understanding that alteration of deep-water formation processes in the North Atlantic fundamentally changed deep circulation globally[70,71,73,127]. But Atlantic Overturning Circulation is only one of the mechanisms controlling carbon sequestration and release during the termination of the LGM. Changes in physical and biological processes in the Southern Ocean described in this Review, and others such as deep ocean carbonate compensation[144], are also required to account for the ocean–atmosphere balance of CO_2 across glacial–interglacial climate periods. We highlight the growing realization that some changes in the Southern Ocean preceded many Northern Hemisphere benchmarks of deglaciation.

The deep southward flow of Atlantic-derived deep water entering the Southern Ocean is widely considered to be a key feature of interglacial climate. Evidence that suggests North Atlantic sourced waters shoaled and were largely restricted from all basins in the deep Southern Ocean until after the ACR. The preponderance of the evidence from the Southern Ocean suggests that a deepening of North Atlantic sourced waters (presuming shoaling lasted until the YD) could not have been a trigger for deglaciation, but was instead a response[239]. Nonetheless, more work determining deep and intermediate water sources is needed to augment available data and solidify this observation.

Warming in mid-latitudes of Southern Hemisphere and Southern Ocean beginning at ~21 ka occurred before the deglacial initiation. The accompanying increases in insolation have led to hypotheses suggesting that insolation could have driven early warming. Although SST data are available from across the several basins in the Southern Ocean, it remains sparse. Given the knowledge that temperature variations vary meridionally and are important in climate forcing[240], more high-resolution time series of SST are needed. Observations of SST targeting frontal locations would improve our very scant knowledge of frontal movements and their timing in the deglaciation. Hard evidence of frontal movements that imply wind shifts are needed to validate mechanisms that have been proposed such as the Zealandia Switch.

The pacing of deglacial atmospheric CO_2 increases in the early deglaciation appears to be in sync with changes in Southern Ocean stratification and ventilation. Ventilation of the deep ocean and formation of shallow water masses are intimately linked to frontal dynamics in the Southern Ocean. In addition to SST observations, there is a need for more information on the timing of changes in deep-water mass chemistry across the basins.

The strategy of combining high-resolution time series and vertical and horizontal transects of the sediment core material from the Pacific[19,180,265] and Atlantic Oceans[70,71,268,101] has been a fundamental tool for establishing that surface and deep conditions in the Southern

Ocean differed from today. Similar sediment core transects from the Indian Ocean basin are needed to improve this picture.

The importance of good chronology across multiple sites using different stratigraphic tools has been vital to constraining the timing of deglacial events across depths, basins and hemispheres. Stratigraphic chronicling of sub-millennial events is critical to understanding climate drivers and requires putting climate proxy records on a common time framework. However, limitations arise when different types of records with independent chronologies are considered collectively without appropriate corrections or cross-correlations. Improved understanding could be gained from compilation of these records, but relies on integrated well-dated and detailed time series, making cross-correlation critical to constraining the relative timing of events. Integration of chronological records is an ongoing effort[269] that should continue to be vigorously pursued.

The role of Southern Ocean in the last deglaciation likely draws on many mechanisms. Numerical model simulations with increasingly higher resolution and better representations of ocean biogeochemistry, ecosystems and sediment processes should continue to be pursued. Constraining the ocean carbon cycle and improving our understanding of the response of Southern Westerly Winds to changes in boundary conditions are the goal. Further research on the impact of Southern Ocean sea-ice changes on global CO_2 is likewise needed.

Published online: 09 June 2023

References

1. Toggweiler, J. R. Variation of atmospheric CO_2 by ventilation of the ocean's deepest water. *Paleoceanography* **14**, 571–588 (1999).
2. Toggweiler, J. R., Russell, J. L. & Carson, J. R. Mid-latitude westerlies, atmospheric CO_2, and climate changes during the ice ages. *Paleoceanography* https://doi.org/10.1029/2005PA001154 (2006).
3. Denton, G. H. et al. The last glacial termination. *Science* **328**, 1652–1656 (2010).
4. Boyle, E. A. Vertical ocean nutrient fractionation and glacial/interglacial CO_2 cycles. *Nature* **331**, 55–56 (1988).
5. Joos, F., Sarmiento, J. L. & Siegenthaler, U. Estimates of the effect of Southern Ocean iron fertilization on atmospheric CO_2 concentrations. *Nature* **349**, 772–775 (1991).
6. Sarmiento, J. L. & Orr, J. C. Three-dimensional simulations of the impact of Southern Ocean nutrient depletion on atmospheric CO_2 and ocean chemistry. *Limnol. Oceanogr.* **36**, 1928–1950 (1991).
7. Denton, G. H. et al. The Zealandia switch: ice age climate shifts viewed from Southern Hemisphere moraines. *Quat. Sci. Rev.* **257**, 106771 (2021).
8. Talley, L. Closure of the global overturning circulation through the Indian, Pacific, and Southern Oceans: schematics and transports. *Oceanography* **26**, 80–97 (2013).
9. Gordon, A. L. South Atlantic thermocline ventilation. *Deep Sea Res.* **28**, 1239–1264 (1981).
10. Marshall, J. & Speer, K. Closure of the Meridional Overturning Circulation through Southern Ocean upwelling. *Nat. Geosci.* **5**, 171–180 (2012).
11. Takahashi, T. et al. Global sea–air CO_2 flux based on climatological surface ocean p CO2, and seasonal biological and temperature effects. *Deep Sea Res. Part II Topical Stud. Oceanogr.* **49**, 1601–1622 (2002).
12. Gray, A. R. et al. Autonomous biogeochemical floats detect significant carbon dioxide outgassing in the high-latitude Southern Ocean. *Geophys. Res. Lett.* **45**, 9049–9057 (2018).
13. Studer, A. S. et al. Increased nutrient supply to the Southern Ocean during the Holocene and its implications for the pre-industrial atmospheric CO_2 rise. *Nat. Geosci.* **11**, 756–760 (2018).
14. Martin, J. H., Gordon, R. M. & Fitzwater, S. E. Iron in Antarctic waters. *Nature* **345**, 156–158 (1990).
15. Kohfeld, K. E. & Chase, Z. Temporal evolution of mechanisms controlling ocean carbon uptake during the last glacial cycle. *Earth Planet. Sci. Lett.* **472**, 206–215 (2017).
16. Sigman, D. M., Hain, M. P. & Haug, G. H. The polar ocean and glacial cycles in atmospheric CO_2 concentration. *Nature* **466**, 47–55 (2010).
17. Ferrari, R. et al. Antarctic sea ice control on ocean circulation in present and glacial climates. *Proc. Natl Acad. Sci. USA* **111**, 8753–8758 (2014).
18. Rae, J. W. B. et al. CO_2 storage and release in the deep Southern Ocean on millennial to centennial timescales. *Nature* **562**, 569–573 (2018).
19. Sikes, E. L., Allen, K. A. & Lund, D. C. Enhanced $\delta^{13}C$ and $\delta^{18}O$ differences between the South Atlantic and South Pacific during the last glaciation: the deep gateway hypothesis. *Paleoceanography* **32**, 1000–1017 (2017).
20. Skinner, L. C., Fallon, S., Waelbroeck, C., Michel, E. & Barker, S. Ventilation of the Deep Southern Ocean and deglacial CO_2 rise. *Science* **328**, 1147–1151 (2010).
21. Menviel, L. et al. Southern Hemisphere westerlies as a driver of the early deglacial atmospheric CO_2 rise. *Nat. Commun.* **9**, 2503 (2018).
22. Marcott, S. A. et al. Centennial-scale changes in the global carbon cycle during the last deglaciation. *Nature* **514**, 616–619 (2014).
23. Shakun, J. D. et al. Global warming preceded by increasing carbon dioxide concentrations during the last deglaciation. *Nature* **484**, 49–54 (2012).
24. Bauska, T. K. et al. Carbon isotopes characterize rapid changes in atmospheric carbon dioxide during the last deglaciation. *Proc. Natl Acad. Sci. USA* **113**, 3465–3470 (2016).
25. Sowers, T., Bender, M., Raynaud, D., Korotkevich, Y. S. & Orchardo, J. The $\delta^{18}O$ of atmospheric O_2 from air inclusions in the Vostok ice core: timing of CO_2 and ice volume changes during the penultimate deglaciation. *Paleoceanography* **6**, 679–696 (1991).
26. Clementi, V. J. & Sikes, E. L. Southwest pacific vertical structure influences on oceanic carbon storage since the last glacial maximum. *Paleoceanogr. Paleoclimatol.* https://doi.org/10.1029/2018PA003501 (2019).
27. Bereiter, B., Shackleton, S., Baggenstos, D., Kawamura, K. & Severinghaus, J. Mean global ocean temperatures during the last glacial transition. *Nature* **553**, 39–44 (2018).
28. Lai, Z., Xu, Y. & Zheng, P. Earth ice age dynamics: a bimodal forcing hypothesis. *Front. Earth Sci.* https://doi.org/10.3389/feart.2021.736895 (2021).
29. Anderson, R. F. et al. Wind-driven upwelling in the Southern Ocean and the deglacial rise in atmospheric CO_2. *Science* **323**, 1441–1448 (2009).
30. Broecker, W. S., Virgilio, A. & Peng, T.-H. Radiocarbon age of waters in the deep Atlantic revisited. *Geophys. Res. Lett.* **18**, 1–3 (1991).
31. Warren, B. A. Suppression of deep oxygen concentrations by Drake Passage. *Deep Sea Res.* **37**, 1899–1907 (1990).
32. Toggweiler, J. R. & Samuels, B. Effect of Drake Passage on the global thermohaline circulation. *Deep Sea Res. I* **42**, 477–500 (1995).
33. Gent, P. R. Effects of Southern Hemisphere wind changes on the meridional overturning circulation in ocean models. *Annu. Rev. Mar. Sci.* **8**, 79–94 (2016).
34. de Lavergne, C., Madec, G., Roquet, F., Holmes, R. M. & McDougall, T. J. Abyssal ocean overturning shaped by seafloor distribution. *Nature* **551**, 181–186 (2017).
35. Rintoul, S. R. The global influence of localized dynamics in the Southern Ocean. *Nature* **558**, 209–218 (2018).
36. Olbers, D., Borowski, D., Völker, C. & Wölff, J.-O. The dynamical balance, transport and circulation of the Antarctic Circumpolar Current. *Antarct. Sci.* **16**, 439–470 (2004).
37. Haumann, F. A., Gruber, N., Münnich, M., Frenger, I. & Kern, S. Sea-ice transport driving Southern Ocean salinity and its recent trends. *Nature* **537**, 89–92 (2016).
38. Sloyan, B. M. & Rintoul, S. R. Circulation, renewal, and modification of Antarctic mode and intermediate water. *J. Phys. Oceanogr.* **31**, 1005–1030 (2001).
39. McCartney, M. S. in *A Voyage of Discovery Deep-Sea Research* (*Suppl.*) Vol. 24 (suppl.) (ed. Angel, M. V.) 103–119 (Pergamon, 1977).
40. Sallée, J.-B., Speer, K., Rintoul, S. & Wijffels, S. Southern Ocean thermocline ventilation. *J. Phys. Oceanogr.* **40**, 509–529 (2010).
41. Polzin, K. L. & Firing, E. Estimates of diapycnal mixing using LADCP and CTD data from I8S. *Int. WOCE Newsl.* **29**, 39–42 (1997).
42. Orsi, A., Whitworth, T. & Nowlin, W. D. On the meridional extent and fronts of the Antarctic Circumpolar Current. *Deep Sea Res.* **42**, 641–673 (1995).
43. Belkin, I. M. & Gordon, A. L. Southern Ocean fronts from the Greenwich meridian to Tasmania. *J. Geophys. Res.* **101**, 3675–3696 (1996).
44. Koch-Larrouy, A., Morrow, R., Penduff, T. & Juza, M. Origin and mechanism of Subantarctic Mode Water formation and transformation in the Southern Indian Ocean. *Ocean Dyn.* **60**, 563–583 (2010).
45. Brady, R. X., Maltrud, M. E., Wolfram, P. J., Drake, H. F. & Lovenduski, N. S. The influence of ocean topography on the upwelling of carbon in the Southern Ocean. *Geophys. Res. Lett.* **48**, e2021GL095088 (2021).
46. Sallée, J. B., Speer, K. G. & Rintoul, S. R. Zonally asymmetric response of the Southern Ocean mixed layer depth to the Southern Annular Mode. *Nat. Geosci.* **3**, 273–279 (2010).
47. Barker, S., Cacho, I., Benway, H. & Tachikawa, K. Planktonic foraminiferal Mg/Ca as a proxy for past oceanic temperatures: a methodological overview and data compilation for the Last Glacial Maximum. *Quat. Sci. Rev.* **24**, 821–834 (2005).
48. Watson, A. J. et al. Rapid cross-density ocean mixing at mid-depths in the Drake Passage measured by tracer release. *Nature* **501**, 408–411 (2013).
49. Tamsitt, V. et al. Spiraling pathways of global deep waters to the surface of the Southern Ocean. *Nat. Commun.* **8**, 172 (2017).
50. Pedro, J. B. et al. Beyond the bipolar seesaw: toward a process understanding of interhemispheric coupling. *Quat. Sci. Rev.* **192**, 27–46 (2018).
51. McDougall, T. J. & Church, J. A. Pitfalls with the numerical representation of isopycnal diapycnal mixing. *J. Phys. Oceanogr.* **16**, 196–199 (1986).
52. Thompson, A. F. & Naveira Garabato, A. C. Equilibration of the Antarctic Circumpolar Current by standing meanders. *J. Phys. Oceanogr.* **44**, 1811–1828 (2014).
53. Kohfeld, K. E. et al. Southern Hemisphere Westerly wind changes during the Last Glacial Maximum: paleo-data synthesis. *Quat. Sci. Rev.* **68**, 76–95 (2013).
54. Martin, J. H., Fitzwater, S. E. & Gordon, R. M. Iron deficiency limits phytoplankton growth in Antarctic waters. *Glob. Biogeochem. Cycles* **4**, 5–12 (1990).
55. Sarmiento, J. L., Gruber, N., Brzezinski, M. A. & Dunne, J. P. High latitude controls on thermocline nutrients and low latitude biological productivity. *Nature* **427**, 56–60 (2004).
56. Moore, C. M. et al. Processes and patterns of oceanic nutrient limitation. *Nat. Geosci.* **6**, 701–710 (2013).

57. Martin, J. H. Glacial–interglacial CO_2 change: the iron hypothesis. *Paleoceanography* **5**, 1–13 (1990).
58. Mitchell, B. G. & Holm-Hansen, O. Observations and modeling of the Antarctic phytoplankton in relation to mixing depth. *Deep Sea Res.* **38**, 981–1007 (1991).
59. Toggweiler, J. R. & Sarmiento, J. L. in *The Carbon Cycle and Atmospheric CO_2: Natural Variations Archean to Present* Vol. 32 (eds Sundquist, E. & Broecker, W. S.) 163–184 (AGU, 1985).
60. Hanawa, K. & Talley, L. D. in *Ocean Circulation and Climate* (eds Seidler, G., Church, J. & Gould, J.) 373–386 (Academic Press, 2001).
61. Williams, R. G., Roussenov, V. & Follows, M. J. Nutrient streams and their induction into the mixed layer. *Global Biogeochem. Cycles* https://doi.org/10.1029/2005GB002586 (2006).
62. Mix, A. C., Bard, E. & Schneider, R. Environmental Processes of the Ice Age: Land, Oceans, Glaciers (EPILOG). *Quat. Sci. Rev.* **20**, 627–657 (2001).
63. Seltzer, A. M. et al. Widespread six degrees Celsius cooling on land during the Last Glacial Maximum. *Nature* **593**, 228–232 (2021).
64. Ruddiman, W. F. & McIntyre, A. The North Atlantic Ocean during the last deglaciation. *Palaeogeogr. Palaeoclimatol. Palaeoecol.* **35**, 145–214 (1981).
65. Sarnthein, M., Pflaumann, U. & Weinelt, M. Past extent of sea ice in the northern North Atlantic inferred from foraminiferal paleotemperature estimates. *Paleoceanography* https://doi.org/10.1029/2002PA000771 (2003).
66. Duplessy, J.-C. et al. Deepwater source variations during the last climatic cycle and their impact on the global deepwater circulation. *Paleoceanography* **3**, 343–360 (1988).
67. Labeyrie, L. D. et al. Changes in the vertical structure of the North Atlantic Ocean between glacial and modern times. *Quat. Sci. Rev.* **11**, 401–413 (1992).
68. Menviel, L. C. et al. Enhanced mid-depth southward transport in the Northeast Atlantic at the last glacial maximum despite a weaker AMOC. *Paleoceanogr. Paleoclimatol.* **35**, e2019PA003793 (2020).
69. Rahmstorf, S. Ocean circulation and climate during the past 120,000 years. *Nature* **419**, 207–214 (2002).
70. Curry, W. B. & Oppo, D. Glacial water mass geometry and the distribution of $\delta^{13}C$ of ΣCO_2 in the Western Atlantic Ocean. *Paleoceanography* **20**, PA1017 (2005).
71. Lund, D. C., Tessin, A. C., Hoffman, J. L. & Schmittner, A. Southwest Atlantic watermass evolution during the last deglaciation. *Paleoceanography* **30**, 477–494 (2015).
72. McManus, J. F., Francois, R., Gherardi, J. M., Keigwin, L. D. & Leger, S. B. Collapse and rapid resumption of Atlantic Meridional Circulation linked to deglacial climate changes. *Nature* **428**, 834–837 (2004).
73. Gherardi, J.-M. et al. Glacial–interglacial circulation changes inferred from $^{231}Pa/^{230}Th$ sedimentary record in the North Atlantic region. *Paleoceanography* **24**, PA2204 (2009).
74. Böhm, E. et al. Strong and deep Atlantic Meridional Overturning Circulation during the last glacial cycle. *Nature* **517**, 73–76 (2015).
75. Gebbie, G. How much did Glacial North Atlantic Water shoal. *Paleoceanography* **29**, 190–209 (2014).
76. Boyle, E. A. & Keigwin, L. D. Comparison of Atlantic and Pacific paleochemical records for the last 215,000 years: changes in deep ocean circulation and chemical inventories. *Earth Planet Sci. Lett.* **76**, 135–150 (1985).
77. Boyle, E. A. & Keigwin, L. D. North Atlantic thermohaline circulation during the past 20,000 years linked to high-latitude surface temperature. *Nature* **330**, 35–40 (1987).
78. Marchitto, T. M. & Broecker, W. S. Deep water mass geometry in the glacial Atlantic Ocean: a review of constraints from the paleonutrient proxy Cd/Ca. *Geochem. Geophys. Geosyst.* https://doi.org/10.1029/2006GC001323 (2006).
79. Charles, C. D., Lynch-Stieglitz, J., Ninnemann, U. S. & Fairbanks, R. G. Climate connections between the hemisphere revealed by deep sea sediment core/ice core correlations. *Earth Planet. Sci. Lett.* **142**, 19–27 (1996).
80. Oppo, D. W. & Fairbanks, R. G. Variability in the deep and intermediate water circulation of the Atlantic Ocean during the past 25,000 years: Northern Hemisphere modulation of the Southern Ocean. *Earth Planet. Sci. Lett.* **86**, 1–15 (1987).
81. Charles, C. D. & Fairbanks, R. G. Evidence from Southern Ocean sediments for the effect of North Atlantic deep-water flux on climate. *Nature* **355**, 416–419 (1992).
82. Ninnemann, U. S. & Charles, C. D. Changes in the mode of Southern Ocean circulation over the last glacial cycle revealed by foraminiferal stable isotopic variability. *Earth Planet. Sci. Lett.* **201**, 383–396 (2002).
83. Muglia, J. & Schmittner, A. Carbon isotope constraints on glacial Atlantic Meridional Overturning: strength vs depth. *Quat. Sci. Rev.* **257**, 106844 (2021).
84. Yu, J. et al. Last glacial atmospheric CO_2 decline due to widespread Pacific deep-water expansion. *Nat. Geosci.* **13**, 628–633 (2020).
85. Noble, T. L., Piotrowskia, M. A. & McCave, I. N. Neodymium isotopic composition of intermediate and deep waters in the glacial southwest Pacific. *Earth Planet. Sci. Lett.* **384**, 27–36 (2013).
86. Williams, T. J. et al. Neodymium isotope evidence for coupled Southern Ocean circulation and Antarctic climate throughout the last 118,000 years. *Quat. Sci. Rev.* **260**, 106915 (2021).
87. Rutberg, R. L., Hemming, S. R. & Goldstein, S. L. Reduced North Atlantic Deep Water flux to the glacial Southern Ocean inferred from neodymium isotope ratios. *Nature* **405**, 935–938 (2000).
88. Piotrowski, A. M., Goldstein, S. L., Hemming, S. R. & Fairbanks, R. G. Temporal relationships of carbon cycling and ocean circulation at glacial boundaries. *Science* **307**, 1933–1938 (2005).
89. Roberts, N. L., Piotrowski, A. M., McManus, J. F. & Keigwin, L. D. Synchronous deglacial overturning and water mass source changes. *Science* **327**, 75–78 (2010).
90. Howe, J. N. et al. North Atlantic deep water production during the last glacial maximum. *Nat. Commun.* **7**, 11765 (2016).
91. Lippold, J. et al. Deep water provenience and dynamics of the (de)glacial Atlantic Meridional Overturning Circulation. *Earth Planet. Sci. Lett.* **445**, 68–78 (2016).
92. Williams, T. J. et al. Paleocirculation and ventilation history of Southern Ocean sourced deep water masses during the last 800,000 years. *Paleoceanogr. Paleoclimatol.* **34**, 833–852 (2019).
93. Ng, H. C. et al. Coherent deglacial changes in western Atlantic Ocean circulation. *Nat. Commun.* **9**, 2947 (2018).
94. Zhao, N. et al. Glacial–interglacial Nd isotope variability of North Atlantic Deep Water modulated by North American ice sheet. *Nat. Commun.* **10**, 5773 (2019).
95. Hu, R. et al. Neodymium isotopic evidence for linked changes in Southeast Atlantic and Southwest Pacific circulation over the last 200 kyr. *Earth Planet. Sci. Lett.* **455**, 106–114 (2016).
96. Basak, C. et al. Breakup of last glacial deep stratification in the South Pacific. *Science* **359**, 900–904 (2018).
97. Wilson, D. J., Piotrowski, A. M., Galy, A. & Banakar, V. K. Interhemispheric controls on deep ocean circulation and carbon chemistry during the last two glacial cycles. *Paleoceanogr. Paleoclimatol.* **30**, 621–641 (2015).
98. Molina-Kescher, M. et al. Reduced admixture of North Atlantic Deep Water to the deep central South Pacific during the last two glacial periods. *Paleoceanography* **31**, 651–668 (2016).
99. Pöppelmeier, F. et al. Water mass gradients of the mid-depth Southwest Atlantic during the past 25,000 years. *Earth Planet. Sci. Lett.* **531**, 115963 (2020).
100. Pavia, F. J., Jones, C. S. & Hines, S. K. Geometry of the Meridional Overturning Circulation at the last glacial maximum. *J. Clim.* **35**, 5465–5482 (2022).
101. Hines, S. K. V. et al. Little change in ice age water mass structure from cape basin benthic neodymium and carbon isotopes. *Paleoceanogr. Paleoclimatol.* **36**, e2021PA004281 (2021).
102. Freeman, E., Skinner, L. C., Waelbroeck, C. & Hodell, D. Radiocarbon evidence for enhanced respired carbon storage in the Atlantic at the Last Glacial Maximum. *Nat. Commun.* **7**, 11998 (2016).
103. Ullermann, J. et al. Pacific–Atlantic circumpolar deep water coupling during the last 500 ka. *Paleoceanogr. Paleoclimatol.* **31**, 639–650 (2016).
104. Piotrowski, A. M. et al. Indian Ocean circulation and productivity during the last glacial cycle. *Earth Planet. Sci. Lett.* **285**, 179–189 (2009).
105. Piotrowski, A. et al. Reconstructing deglacial North and South Atlantic deep water sourcing using foraminiferal Nd isotopes. *Earth Planet. Sci. Lett.* **357**, 289–297 (2012).
106. McCave, I. N., Carter, L. & Hall, I. R. Glacial–interglacial changes in water mass structure and flow in the SW Pacific Ocean. *Quat. Sci. Rev.* **27**, 1886–1908 (2008).
107. Huang, H., Gutjahr, M., Eisenhauer, A. & Kuhn, G. No detectable Weddell Sea Antarctic Bottom Water export during the last and penultimate glacial maximum. *Nat. Commun.* **11**, 424 (2020).
108. Hodell, D. A., Venz, K. A., Charles, C. D. & Ninnemann, U. S. Pleistocene vertical carbon isotope and carbonate gradients in the South Atlantic sector of the Southern Ocean. *Geochem. Geophys. Geosyst.* **4**, 1004 (2003).
109. Sikes, E. L., Elmore, A. C., Cook, M. S., Allen, K. A. & Guilderson, T. P. Glacial water mass structure and rapid $\delta^{18}O$ and $\delta^{13}C$ changes during the last glacial termination in the Southwest Pacific. *Earth Planet. Sci. Lett.* **456**, 87–97 (2016).
110. Ronge, T. A. et al. Pushing the boundaries: glacial/interglacial variability of intermediate and deep waters in the southwest Pacific over the last 350,000 years. *Paleoceanography* **30**, 23–38 (2015).
111. Curry, W. B., Duplessy, J.-C., Labeyrie, L. D. & Shackleton, N. J. Changes in the distribution of $\delta^{13}C$ of deep water ΣCO_2 between the last glaciation and the Holocene. *Paleoceanography* **3**, 317–341 (1988).
112. Charles, C. D. et al. Millennial scale evolution of the Southern Ocean chemical divide. *Quat. Sci. Rev.* **29**, 399–409 (2010).
113. Allen, K. A., Sikes, E. L., Anderson, R. F. & Rosenthal, Y. Rapid loss of CO_2 from the South Pacific Ocean during the last glacial termination. *Paleoceanogr. Paleoclimatol.* **35**, 2019PA003766 (2020).
114. Kallel, N., Labeyrie, L. D., Juillet-Leclerc, A. & Duplessy, J.-C. A deep hydrological front between intermediate and deep-water masses in the glacial Indian Ocean. *Nature* **333**, 651–655 (1988).
115. McCorkle, D. C., Heggie, D. T. & Veeh, H. H. Glacial and Holocene stable isotopic distributions in the southeastern Indian Ocean. *Paleoceanography* **13**, 20–34 (1998).
116. Lacerra, M., Lund, D., Yu, J. & Schmittner, A. Carbon storage in the mid-depth Atlantic during millennial-scale climate events: mid-depth Atlantic Carbon Storage. *Paleoceanography* https://doi.org/10.1002/2016PA003081 (2017).
117. Hines, S. K. V., Southon, J. R. & Adkins, J. F. A high-resolution record of Southern Ocean intermediate water radiocarbon over the past 30,000 years. *Earth Planet. Sci. Lett.* **432**, 46–58 (2015).
118. Burke, A. & Robinson, L. F. The Southern Ocean's role in carbon exchange during the Last Deglaciation A. *Science* **335**, 557–561 (2012).
119. Sikes, E. L., Samson, C. R., Guilderson, T. P. & Howard, W. R. Old radiocarbon ages in the southwest Pacific Ocean during the last glacial period and deglaciation. *Nature* **405**, 555–559 (2000).
120. Sikes, E. L., Cook, M. S. & Guilderson, T. P. Reduced deep ocean ventilation in the Southern Pacific Ocean during the last glaciation persisted into the deglaciation. *Earth Planet. Sci. Lett.* **438**, 130–138 (2016).

121. Ronge, T. A. et al. Radiocarbon constraints on the extent and evolution of the South Pacific glacial carbon pool. *Nat. Commun.* https://doi.org/10.1038/ncomms11487 (2016).
122. Dai, Y., Yu, J. & Rafter, P. Deglacial ventilation changes in the Deep Southwest Pacific. *Paleoceanogr. Paleoclimatol.* https://doi.org/10.1029/2020PA004172 (2021).
123. Meissner, K. J., Schmittner, A., Weaver, A. J. & Adkins, J. F. Ventilation of the North Atlantic Ocean during the Last Glacial Maximum: a comparison between simulated and observed radiocarbon ages. *Paleoceanography* **18**, 1023 (2003).
124. Menviel, L. et al. Poorly ventilated deep ocean at the Last Glacial Maximum inferred from carbon isotopes: a data-model comparison study. *Paleoceanography* **32**, 2–17 (2017).
125. Skinner, L. et al. Reduced ventilation and enhanced magnitude of the deep Pacific carbon pool during the last glacial period. *Earth Planet. Sci. Lett.* **411**, 45–52 (2015).
126. Skinner, L. C. et al. Radiocarbon constraints on the glacial ocean circulation and its impact on atmospheric CO_2. *Nat. Commun.* **8**, 16010 (2017).
127. Robinson, L. F. et al. Radiocarbon variability in the western North Atlantic during the last deglaciation. *Science* **310**, 1469–1473 (2005).
128. Adkins, J. F., Cheng, H., Boyle, E. A., Druffel, E. R. M. & Edwards, R. L. Deep-sea coral evidence for rapid change in ventilation of the deep North Atlantic 15,400 years ago. *Science* **280**, 725–728 (1998).
129. Broecker, W. S. Glacial to interglacial changes in ocean chemistry. *Prog. Oceanogr.* **11**, 151–197 (1982).
130. Martínez Fontaine, C. et al. Ventilation of the deep ocean carbon reservoir during the last deglaciation: results from the Southeast Pacific. *Paleoceanogr. Paleoclimatol.* **34**, 2080–2097 (2019).
131. Keigwin, L. D. & Lehman, S. J. Radiocarbon evidence for a possible abyssal front near 3.1km in the glacial equatorial Pacific Ocean. *Earth Planet. Sci. Lett.* **425**, 93–104 (2015).
132. de la Fuente, M., Skinner, L., Calvo, E., Pelejero, C. & Cacho, I. Increased reservoir ages and poorly ventilated deep waters inferred in the glacial Eastern Equatorial Pacific. *Nat. Commun.* **6**, 7420 (2015).
133. Umling, N. E. & Thunell, R. C. Synchronous deglacial thermocline and deep-water ventilation in the eastern equatorial Pacific. *Nat. Commun.* **8**, 14203 (2017).
134. Ronge, T. A. et al. Radiocarbon evidence for the contribution of the Southern Indian Ocean to the evolution of atmospheric CO_2 over the last 32,000 years. *Paleoceanogr. Paleoclimatol.* **35**, e2019PA003733 (2020).
135. Gottschalk, J. et al. Glacial heterogeneity in Southern Ocean carbon storage abated by fast South Indian deglacial carbon release. *Nat. Commun.* **11**, 6192 (2020).
136. Bharti, N. et al. Evidence of poorly ventilated deep Central Indian Ocean during the last glaciation. *Earth Planet. Sci. Lett.* **582**, 117438 (2022).
137. Ronge, T. A. et al. Radiocarbon evidence for the contribution of the Southern Indian Ocean to the evolution of atmospheric CO_2 over the last 32,000 years. *Paleoceanogr. Paleoclimatol.* **35**, e2019PA003733 (2019).
138. Rose, K. R. et al. Upper-ocean-to-atmosphere radiocarbon offsets imply fast deglacial carbon dioxide release. *Nature* **466**, 1093–1097 (2010).
139. Sortor, R. N. & Lund, D. C. No evidence for a deglacial intermediate water delta C-14 anomaly in the SW Atlantic. *Earth Planet. Sci. Lett.* **310**, 65–72 (2011).
140. Siani, G. et al. Carbon isotope records reveal precise timing of enhanced Southern Ocean upwelling during the last deglaciation. *Nat. Commun.* **4**, 2758 27 (2013).
141. Chen, T. et al. Synchronous centennial abrupt events in the ocean and atmosphere during the last deglaciation. *Science* **349**, 1537–1541 (2015).
142. Chen, T. et al. Persistently well-ventilated intermediate-depth ocean through the last deglaciation. *Nat. Geosci.* **13**, 733–738 (2020).
143. Adkins, J. F. The role of deep ocean circulation in setting glacial climates. *Paleoceanography* **28**, 1–23 (2013).
144. Boyle, E. A. The role of vertical chemical fractionation in controlling late Quaternary atmospheric carbon dioxide. *J. Geophys. Res.* **93**, 15701–15714 (1988).
145. Skinner, L. C. Glacial–interglacial atmospheric CO_2 change: a possible 'standing volume' effect on deep-ocean carbon sequestration. *Clim. Past* **5**, 537–550 (2009).
146. Hain, M. P., Sigman, D. M. & Haug, G. H. Carbon dioxide effects of Antarctic stratification, North Atlantic Intermediate Water formation, and Subantarctic nutrient drawdown during the last ice age: diagnosis and synthesis in a geochemical box model. *Glob. Biogeochem. Cycles* **24**, GB4023 (2010).
147. Anderson, R. F. et al. Biological response to millennial variability of dust and nutrient supply in the Subantarctic South Atlantic Ocean. *Phil. Trans. R. Soc. A* **372**, 20130054 (2014).
148. Kohfeld, K. E. Role of marine biology in glacial–interglacial CO_2 cycles. *Science* **308**, 74–78 (2005).
149. Martinez-Garcia, A. et al. Iron fertilization of the Subantarctic Ocean during the last ice age. *Science* **343**, 1347–1350 (2014).
150. Chase, Z., Anderson, R. F. & Fleisher, M. Q. Evidence from authigenic uranium for increased productivity of the glacial Subantarctic Ocean. *Paleoceanography* **16**, 468–478 (2001).
151. Kumar, N. et al. Increased biological productivity and export production in the glacial Southern Ocean. *Nature* **378**, 675–680 (1995).
152. Francois, R. et al. Contribution of Southern Ocean surface-water stratification to low atmospheric CO_2 concentrations during the last glacial period. *Nature* **389**, 929–935 (1997).
153. Jaccard, S. L., Galbraith, E. D., Martínez-García, A. & Anderson, R. F. Covariation of deep Southern Ocean oxygenation and atmospheric CO_2 through the last ice age. *Nature* **530**, 207–210 (2016).
154. Mortlock, R. A. et al. Evidence for lower productivity in the Antarctic Ocean during the last glaciation. *Nature* **351**, 220–223 (1991).
155. Charles, C. D., Froelich, P. N., Zibello, M. A., Mortlock, R. A. & Morley, J. J. Biogenic opal in Southern Ocean sediments over the last 450,000 years: implications for surface water chemistry and circulation. *Paleoceanography* **6**, 697–728 (1991).
156. Chase, Z., Anderson, R. F., Fleisher, M. Q. & Kubik, P. W. Accumulation of biogenic and lithogenic material in the Pacific sector of the Southern Ocean during the past 40,000 years. *Deep Sea Res. II* **50**, 799–832 (2003).
157. Kumar, N., Gwiazda, R., Anderson, R. F. & Froelich, P. N. $^{231}Pa/^{230}Th$ ratios in sediments as a proxy for past changes in Southern Ocean productivity. *Nature* **362**, 45–48 (1993).
158. Sigman, D. M. et al. The Southern Ocean during the ice ages: a review of the Antarctic surface isolation hypothesis, with comparison to the North Pacific. *Quat. Sci. Rev.* **254**, 106732 (2021).
159. Ai, X. E. et al. Southern Ocean upwelling, Earth's obliquity, and glacial–interglacial atmospheric CO_2 change. *Science* **370**, 1348–1352 (2020).
160. Robinson, R. S. & Sigman, D. M. Nitrogen isotopic evidence for a poleward decrease in surface nitrate within the ice age Antarctic. *Quat. Sci. Rev.* **27**, 1076–1090 (2008).
161. Studer, A. S. et al. Antarctic Zone nutrient conditions during the last two glacial cycles. *Paleoceanography* **30**, 845–862 (2015).
162. Saini, H. et al. Southern Ocean ecosystem response to last glacial maximum boundary conditions. *Paleoceanogr. Paleoclimatol.* **36**, e2020PA004075 (2021).
163. Jaccard, S. L. & Galbraith, E. D. Direct ventilation of the North Pacific did not reach the deep ocean during the last deglaciation. *Geophys. Res. Lett.* **40**, 199–203 (2013).
164. Yamamoto, A., Abe-Ouchi, A., Ohgaito, R., Ito, A. & Oka, A. Glacial CO_2 decrease and deep-water deoxygenation by iron fertilization from glaciogenic dust. *Clim. Past* **15**, 981–996 (2019).
165. Muglia, J., Skinner, L. C. & Schmittner, A. Weak overturning circulation and high Southern Ocean nutrient utilization maximized glacial ocean carbon. *Earth Planet. Sci. Lett.* **496**, 47–56 (2018).
166. Cliff, E., Khatiwala, S. & Schmittner, A. Glacial deep ocean deoxygenation driven by biologically mediated air–sea disequilibrium. *Nat. Geosci.* **14**, 43–50 (2021).
167. Anderson, R. F. et al. Deep-sea oxygen depletion and ocean carbon sequestration during the last ice age. *Glob. Biogeochem. Cycles* **33**, 301–317 (2019).
168. Rodrigo-Gámiz, M., Rampen, S. W., Schouten, S. & Sinninghe Damsté, J. S. The impact of oxic degradation on long chain alkyl diol distributions in Arabian Sea surface sediments. *Org. Geochem.* **100**, 1–9 (2016).
169. Hoogakker, B. A. A., Elderfield, H., Schmiedl, G., McCave, I. N. & Rickaby, R. E. M. Glacial–interglacial changes in bottom-water oxygen content on the Portuguese margin. *Nat. Geosci.* **8**, 40–43 (2014).
170. McCorkle, D. C. & Emerson, S. R. The relationship between pore water carbon isotopic composition and bottom water oxygen concentration. *Geochim. Cosmochim. Acta* **52**, 1169–1178 (1988).
171. Hoogakker, B. A. A. et al. Glacial expansion of oxygen-depleted seawater in the eastern tropical Pacific. *Nature* **562**, 410–413 (2018).
172. Jacobel, A. W. et al. Deep Pacific storage of respired carbon during the last ice age: perspectives from bottom water oxygen reconstructions. *Quat. Sci. Rev.* **230**, 106065 (2020).
173. Jaccard, S. L. et al. Subarctic Pacific evidence for a glacial deepening of the oceanic respired carbon pool. *Earth Planet. Sci. Lett.* **277**, 156–165 (2009).
174. Sarnthein, M., Schneider, B. & Grootes, P. M. Peak glacial ^{14}C ventilation ages suggest major draw-down of carbon into the abyssal ocean. *Clim. Past* **9**, 2595–2614 (2013).
175. Schmittner, A. & Somes, C. J. Complementary constraints from carbon (^{13}C) and nitrogen (^{15}N) isotopes on the glacial ocean's soft-tissue biological pump. *Paleoceanography* **31**, 669–693 (2016).
176. Bradtmiller, L. I., Anderson, R. F., Sachs, J. P. & Fleisher, M. Q. A deeper respired carbon pool in the glacial equatorial Pacific Ocean. *Earth Planet. Sci. Lett.* **299**, 417–425 (2010).
177. Jaccard, S. L. & Galbraith, E. D. Large climate-driven changes of oceanic oxygen concentrations during the last deglaciation. *Nat. Geosci.* **5**, 151–156 (2011).
178. Keeling, R. F. & Stephens, B. B. Antarctic sea ice and the control of Pleistocene climate instability. *Paleoceanography* **16**, 112–131 (2001).
179. Sarmiento, J. L. & Toggweiler, J. R. A new model for the role of the oceans in determining atmospheric pCO_2. *Nature* **308**, 621–624 (1984).
180. Sikes, E. L. et al. Southern Ocean seasonal temperature and Subtropical Front movement on the South Tasman Rise in the late Quaternary. *Paleoceanography* **24**, PA2201 (2009).
181. Moros, M. et al. Hydrographic shifts south of Australia over the last deglaciation and possible interhemispheric linkages. *Quat. Res.* **102**, 130–141 (2021).
182. Peeters, F. J. C. et al. Vigorous exchange between the Indian and Atlantic oceans at the end of the past five glacial periods. *Nature* **430**, 661–665 (2004).
183. Ferry, A. J. et al. First records of winter sea ice concentration in the southwest Pacific sector of the Southern Ocean. *Paleoceanography* **30**, 1525–1539 (2015).
184. WAIS, D. P. M. et al. Onset of deglacial warming in West Antarctica driven by local orbital forcing. *Nature* **500**, 440–444 (2013).
185. Gersonde, R., Crosta, X., Abelmann, A. & Armand, L. Sea-surface temperature and sea ice distribution of the Southern Ocean at the EPILOG Last Glacial Maximum — a circum-Antarctic view based on siliceous microfossil records. *Quat. Sci. Rev.* **24**, 869–896 (2005).
186. Benz, V., Esper, O., Gersonde, R., Lamy, F. & Tiedemann, R. Last Glacial Maximum sea surface temperature and sea-ice extent in the Pacific sector of the Southern Ocean. *Quat. Sci. Rev.* **146**, 216–237 (2016).
187. Green, R. A. et al. Evaluating seasonal sea-ice cover over the Southern Ocean at the Last Glacial Maximum. *Clim. Past* **18**, 845–862 (2022).

188. Prend, C. J. et al. Indo-Pacific sector dominates southern ocean carbon outgassing. *Glob. Biogeochem. Cycles* **36**, e2021GB007226 (2022).
189. Russell, J. L., Dixon, K. W., Gnanadesikan, A., Stouffer, R. J. & Toggweiler, J. R. Southern Ocean Westerlies in a warming world: propping open the door to the deep ocean. *J. Clim.* **19**, 6382–6390 (2006).
190. CLIMAP. *Seasonal Reconstructions of the Earth's Surface at the Last Glacial Maximum* (ed. Cline, R.) (Geological Society of America, 1981).
191. Trend-Staid, M. & Prell, W. L. Sea surface temperature at the Last Glacial Maximum: a reconstruction using the modern analog technique. *Paleoceanography* https://doi.org/10.1029/2000PA000506 (2002).
192. Sikes, E. L., Howard, W. R., Neil, H. L. & Volkman, J. K. Glacial–interglacial sea surface temperature changes across the subtropical front east of New Zealand based on alkenone unsaturation ratios and foraminiferal assemblages. *Paleoceanography* https://doi.org/10.1029/2001PA000640 (2002).
193. Pahnke, K. & Sachs, J. P. Sea surface temperatures of southern midlatitudes 0–160 kyr B.P. *Paleoceanography* **21**, PA2003 (2006).
194. Moy, A. D. et al. Varied contribution of the Southern Ocean to deglacial atmospheric CO_2 rise. *Nat. Geosci.* **12**, 1006–1011 (2019).
195. Ikehara, M. et al. Alkenone sea surface temperature in the Southern Ocean for the last two deglaciations. *Geophys. Res. Lett.* **24**, 679–682 (1997).
196. Sikes, E. L., Schiraldi, B. & Williams, A. Seasonal and latitudinal response of New Zealand sea surface temperature to warming climate since the last glaciation: comparing alkenones to Mg/Ca foraminiferal reconstructions. *Paleoceanogr. Paleoclimatol.* https://doi.org/10.1029/2019PA003649 (2019).
197. Sikes, E. L., Nodder, S. D., O'Leary, T. & Volkman, J. K. Alkenone temperature records and biomarker flux at the subtropical front on the Chatham Rise, SW Pacific Ocean. *Deep Sea Res. I* **52**, 721–748 (2005).
198. Bostock, H. C., Hayward, B. W., Neil, H. L., Sabaa, A. T. & Scott, G. H. Changes in the position of the Subtropical Front south of New Zealand since the last glacial period. *Paleoceanography* **30**, 824–844 (2015).
199. Bard, E. & Rickaby, R. E. M. Migration of the subtropical front as a modulator of glacial climate. *Nature* **460**, 380–384 (2009).
200. Howard, W. R. & Prell, W. L. Late Quaternary surface circulation of the Southern Indian Ocean and its relationship to orbital variations. *Paleoceanography* **7**, 79–118 (1992).
201. Civel-Mazens, M. et al. Antarctic Polar Front migrations in the Kerguelen Plateau region, Southern Ocean, over the past 360 kyrs. *Glob. Planet. Change* **202**, 103526 (2021).
202. De Deckker, P., Moros, M., Perner, K. & Jansen, E. Influence of the tropics and southern westerlies on glacial interhemispheric asymmetry. *Nat. Geosci.* **5**, 266–269 (2012).
203. Lamy, F., Kaiser, J., Ninnemann, U., Hebbeln, D., Arz, H. W. & Stoner, J. Antarctic timing of surface water changes off Chile and Patagonian ice sheet response. *Science* **304**, 1959–1962 (2004).
204. Wells, P. E. & Connell, R. Movement of hydrological fronts and widespread erosional events in the southwestern Tasman Sea during the Late Quaternary. *Austr. J. Earth Sci.* **44**, 105–112 (1997).
205. Lynch-Stieglitz, J., Fairbanks, R. G. & Charles, C. D. Glacial–interglacial history of Antarctic Intermediate Water: relative strengths of Antarctic versus Indian Ocean sources. *Paleoceanography* **9**, 7–29 (1994).
206. Allison, L. C., Johnson, H. L., Marshall, D. P. & Munday, D. R. Where do winds drive the Antarctic Circumpolar Current? *Geophys. Res. Lett.* https://doi.org/10.1029/2010GL043355 (2010).
207. Wang, J., Mazloff, M. R. & Gille, S. T. The effect of the Kerguelen Plateau on the ocean circulation. *J. Phys. Oceanogr.* **46**, 3385–3396 (2016).
208. Sikes, E. L., Medeiros, P. M., Augustinas, P., Wilmshurst, J. & Freeman, K. Seasonal variations in aridity and temperature characterize changing climate during the last deglaciation in New Zealand. *Quat. Sci. Rev.* **74**, 246–256 (2013).
209. Newnham, R. M. et al. Does the bipolar seesaw extend to the terrestrial southern mid-latitudes? *Quat. Sci. Rev.* **36**, 214–222 (2012).
210. Turney, C. S. M. et al. Climatic variability in the southwest Pacific during the Last Termination (20–10 kyr BP). *Quat. Sci. Rev.* **25**, 886–903 (2006).
211. McGlone, M. S., Turney, C. S. M., Wilmshurst, M. J., Renwick, J. & Pahnke, K. Divergent trends in land and ocean temperature in the Southern Ocean over the past 18,000 years. *Nat. Geosci.* **3**, 622–626 (2010).
212. d'Orgeville, M., Sijp, W. P., England, M. H. & Meissner, K. J. On the control of glacial–interglacial atmospheric CO_2 variations by the Southern Hemisphere westerlies. *Geophys. Res. Lett.* https://doi.org/10.1029/2010GL045261 (2010).
213. Huiskamp, W. N., Meissner, K. J. & d'Orgeville, M. Competition between ocean carbon pumps in simulations with varying Southern Hemisphere westerly wind forcing. *Clim. Dyn.* **46**, 3463–3480 (2016).
214. Gottschalk, J. et al. Mechanisms of millennial-scale atmospheric CO_2 change in numerical model simulations. *Quat. Sci. Rev.* **220**, 30–74 (2019).
215. Marzocchi, A. & Jansen, M. F. Global cooling linked to increased glacial carbon storage via changes in Antarctic sea ice. *Nat. Geosci.* **12**, 1001–1005 (2019).
216. Beadling, R. L. et al. Representation of Southern Ocean properties across coupled model Intercomparison Project Generations: CMIP3 to CMIP6. *J. Clim.* **33**, 6555–6581 (2020).
217. Bronselaer, B. et al. Importance of wind and meltwater for observed chemical and physical changes in the Southern Ocean. *Nat. Geosci.* **13**, 35–42 (2020).
218. Sigman, D. M. & Boyle, E. A. Glacial/interglacial variations in atmospheric carbon dioxide. *Nature* **407**, 859–869 (2000).
219. Fairbanks, R. G. A 17,000-year glacio-eustatic sea level record: influence of glacial melting rates on the Younger Dryas event and deep-ocean circulation. *Nature* **342**, 637–642 (1989).
220. Rasmussen, S. O. et al. A stratigraphic framework for abrupt climatic changes during the Last Glacial period based on three synchronized Greenland ice-core records: refining and extending the INTIMATE event stratigraphy. *Quat. Sci. Rev.* **106**, 14–28 (2014).
221. Brook, E. J., Harder, S., Severinghaus, J., Steig, E. J. & Sucher, C. M. On the origin and timing of rapid changes in atmospheric methane during the last glacial period. *Glob. Biogeochem. Cycles* **14**, 559–572 (2000).
222. Wang, Y. J. et al. A high-resolution absolute-dated Late Pleistocene Monsoon Record from Hulu Cave, China. *Science* **294**, 2345–2348 (2001).
223. Reimer, P. J. et al. IntCal13 and Marine13 radiocarbon age calibration curves 0–50,000 years cal BP. *Radiocarbon* **55**, 1869–1887 (2013).
224. Alloway, B. V. et al. Towards a climate event stratigraphy for New Zealand over the past 30,000 years (NZ-INTIMATE project). *J. Quat. Sci.* **22**, 9–35 (2007).
225. Stocker, T. F. & Johnsen, S. J. A minimum thermodynamic model for the bipolar seesaw. *Paleoceanography* https://doi.org/10.1029/2003PA000920 (2003).
226. Landais, A. et al. A review of the bipolar see–saw from synchronized and high resolution ice core water stable isotope records from Greenland and East Antarctica. *Quat. Sci. Rev.* **114**, 18–32 (2015).
227. Broecker, W. S. Paleocean circulation during the last deglaciation: a biopolar seesaw? *Paleoceanography* **13**, 119–121 (1998).
228. Denton, G. H., Toucanne, S., Putnam, A. E., Barrell, D. J. A. & Russell, J. L. Heinrich summers. *Quat. Sci. Rev.* **295**, 107750 (2022).
229. Monnin, E. et al. Atmospheric CO_2 concentrations over the Last Glacial Termination. *Science* **291**, 112–114 (2001).
230. Denton, G., Alley, R., Comer, G. & Broecker, W. The role of seasonality in abrupt climate change. *Quat. Sci. Rev.* **24**, 1159–1182 (2005).
231. He, C. et al. Abrupt Heinrich Stadial 1 cooling missing in Greenland oxygen isotopes. *Sci. Adv.* **7**, eabh1007 (2021).
232. Sowers, T. & Bender, M. Climate records covering the last deglaciation. *Science* **269**, 210–213 (1995).
233. Huybers, P. & Denton, G. Antarctic temperature at orbital timescales controlled by local summer duration. *Nat. Geosci.* **1**, 787–792 (2008).
234. Stott, L., Timmermann, A. & Thunell, R. Southern hemisphere and deep-sea warming led deglacial atmospheric CO_2 rise and tropical warming. *Science* **318**, 435–438 (2007).
235. Samson, C. R., Sikes, E. L. & Howard, W. R. Deglacial paleoceanographic history of the Bay of Plenty, New Zealand. *Paleoceanography* https://doi.org/10.1029/2004PA001088 (2005).
236. Kumar, V., Tiwari, M., Prakash, P., Mohan, R. & Thamban, M. SST changes in the Indian sector of the Southern Ocean and their teleconnection with the Indian monsoon during the last glacial period. *Paleoceanogr. Paleoclimatol.* **36**, e2020PA004139 (2021).
237. Shukla, S. K., Crosta, X. & Ikehara, M. Sea surface temperatures in the Indian sub-Antarctic Southern Ocean for the Last Four Interglacial Periods. *Geophys. Res. Lett.* **48**, e2020GL090994 (2021).
238. Parrenin, F. et al. Synchronous change of atmospheric CO_2 and Antarctic temperature during the last deglacial warming. *Science* **339**, 1060–1063 (2013).
239. Chowdhry Beeman, J. et al. Antarctic temperature and CO_2: near-synchrony yet variable phasing during the last deglaciation. *Clim. Past* **15**, 913–926 (2019).
240. Lamy, F. et al. Precession modulation of the South Pacific westerly wind belt over the past million years. *Proc. Natl Acad. Sci. USA* **116**, 23455–23460 (2019).
241. Menviel, L. C., Skinner, L. C., Tarasov, L. & Tzedakis, P. C. An ice–climate oscillatory framework for Dansgaard–Oeschger cycles. *Nat. Rev. Earth Environ.* **1**, 677–693 (2020).
242. Knorr, G. & Lohmann, G. Southern Ocean origin for the resumption of Atlantic thermocline circulation during deglaciation. *Nature* **424**, 532–536 (2003).
243. Buizert, C. et al. Abrupt ice-age shifts in southern westerly winds and Antarctic climate forced from the north. *Nature* **563**, 681–685 (2018).
244. Schiraldi, B., Sikes, E. L., Elmore, A. C., Cook, M. S. & Rose, K. A. Southwest Pacific subtropics responded to last deglacial warming with changes in shallow water sources. *Paleoceanography* https://doi.org/10.1002/2013PA002584 (2014).
245. Basak, C., Pahnke, K., Frank, M., Lamy, F. & Gersonde, R. Neodymium isotopic characterization of Ross Sea Bottom Water and its advection through the southern South Pacific. *Earth Planet. Sci. Lett.* **419**, 211–221 (2015).
246. Pöppelmeier, F. et al. Stable Atlantic deep water mass sourcing on glacial–interglacial timescales. *Geophys. Res. Lett.* **48**, e2021GL092722 (2021).
247. Du, J., Haley, B. A., Mix, A. C., Walczak, M. H. & Praetorius, S. K. Flushing of the deep Pacific Ocean and the deglacial rise of atmospheric CO_2 concentrations. *Nat. Geosci.* **11**, 749–755 (2018).
248. Elderfield, H. et al. A record of bottom water temperature and seawater $\delta^{18}O$ for the Southern Ocean over the past 440 kyr based on Mg/Ca of benthic foraminiferal *Uvigerina* spp. *Quat. Sci. Rev.* **29**, 160–169 (2010).
249. Elderfield, H. et al. Evolution of ocean temperature and ice volume through the mid-Pleistocene climate transition. *Science* **337**, 704–709 (2012).
250. Zhao, N., Marchal, O., Keigwin, L., Amrhein, D. & Gebbie, G. A synthesis of deglacial deep-sea radiocarbon records and their (In)consistency with modern ocean ventilation. *Paleoceanogr. Paleoclimatol.* **33**, 128–151 (2018).
251. Mangini, A. et al. Deep sea corals off Brazil verify a poorly ventilated Southern Pacific Ocean during H2, H1 and the Younger Dryas. *Earth Planet. Sci. Lett.* **293**, 269–276 (2010).

252. Marchitto, T., Lehman, S. J., Ortiz, J. D., Flückiger, J. & vanGeen, A. Marine radiocarbon evidence for the mechanism of deglacial atmospheric CO_2 rise. *Science* **316**, 1456–1459 (2007).
253. Thornalley, D. J. R., Barker, S., Broecker, W. S., Elderfield, H. & McCave, I. N. The deglacial evolution of North Atlantic deep convection. *Science* **331**, 202–205 (2011).
254. van Geen, A., Fairbanks, R. G., Dartnell, P., McGann, M. & Gardner, J. V. Ventilation changes in the northeast Pacific during the last deglaciation. *Paleoceanography* **11**, 519–528 (1996).
255. Bryan, S. P., Marchitto, T. M. & Lehman, S. J. The release of 14C-depleted carbon from the deep ocean during the last deglaciation: evidence from the Arabian Sea. *Earth Planet. Sci. Lett.* **298**, 244–254 (2010).
256. Stott, L. No signs of Southern Ocean CO_2. *Nat. Geosci.* **3**, 153–154 (2010).
257. Martínez-Botí, M. A. et al. Boron isotope evidence for oceanic carbon dioxide leakage during the last deglaciation. *Nature* **518**, 219–222 (2015).
258. Kubota, K., Yokoyama, Y., Ishikawa, T., Obrochta, S. & Suzuki, A. Larger CO_2 source at the equatorial Pacific during the last deglaciation. *Sci. Rep.* https://doi.org/10.1038/srep05261 (2015).
259. Kubota, K. et al. Equatorial Pacific seawater pCO_2 variability since the last glacial period. *Sci. Rep.* **9**, 13814 (2019).
260. Li, T. et al. Rapid shifts in circulation and biogeochemistry of the Southern Ocean during deglacial carbon cycle events. *Sci. Adv.* **6**, eabb3807 (2020).
261. Galbraith, E. D., Kienast, M., Pedersen, T. F. & Calvert, S. E. Glacial–interglacial modulation of the marine nitrogen cycle by high-latitude O_2 supply to the global thermocline. *Paleoceanography* https://doi.org/10.1029/2003PA001000 (2004).
262. Robinson, R. S., Martinez, P., Pena, L. D. & Cacho, I. Nitrogen isotopic evidence for deglacial changes in nutrient supply in the eastern equatorial Pacific. *Paleoceanography* https://doi.org/10.1029/2008PA001702 (2009).
263. Robinson, R. S., Brunelle, B. G. & Sigman, D. M. Revisiting nutrient utilization in the glacial Antarctic: evidence from a new method for diatom-bound N isotopic analysis. *Paleoceanography* **19**, PA3001 (2004).
264. Lamy, F. et al. Increased dust deposition in the Pacific Southern Ocean during glacial periods. *Science* **343**, 403–407 (2014).
265. Thöle, L. M. et al. Glacial–interglacial dust and export production records from the Southern Indian Ocean. *Earth Planet. Sci. Lett.* **525**, 115716 (2019).
266. Le Quéré, C. et al. Global Carbon Budget 2018. *Earth Syst. Sci. Data* **10**, 2141–2194 (2018).
267. Broecker, W. S. Ocean chemistry during glacial time. *Geochim. Cosmochim. Acta* **46**, 1689–1705 (1982).
268. Repschläger, J. et al. Active North Atlantic deepwater formation during Heinrich Stadial 1. *Quat. Sci. Rev.* **270**, 107145 (2021).
269. Guilderson, T. P., Allen, K., Landers, J. P., Ettwein, V. J. & Cook, M. S. Can we better constrain the timing of GNAIW/UNADW variability in the western equatorial atlantic and its relationship to climate change during the last deglaciation? *Paleoceanogr. Paleoclimatol.* **36**, e2020PA004187 (2021).
270. Schmittner, A. et al. Calibration of the carbon isotope composition ($\delta^{13}C$) of benthic foraminifera. *Paleoceanography* **32**, 512–530 (2017).
271. Lumpkin, R. & Speer, K. Global ocean meridional overturning. *J. Phys. Oceanogr.* **37**, 2550–2562 (2007).
272. Heinrich, H. Origin and consequences of cyclic ice rafting in the Northeast Atlantic Ocean during the past 130,000 years. *Quat. Res.* **29**, 142–152 (1988).
273. Dansgaard, W. et al. Evidence for general instability of past climate from a 250-kyr ice-core record. *Nature* **364**, 218–220 (1993).
274. Barker, S. et al. Interhemispheric Atlantic seesaw response during the last deglaciation. *Nature* **457**, 1097–1102 (2009).
275. Hodell, D. A. et al. Anatomy of Heinrich Layer 1 and its role in the last deglaciation. *Paleoceanography* **32**, 284–303 (2017).
276. McManus, J., Berelson, W. M., Klinkhammer, G. P., Hammond, D. E. & Holm, C. Authigenic uranium: relationship to oxygen penetration depth and organic carbon rain. *Geochim. Cosmochim. Acta* **69**, 95–108 (2005).
277. Wang, Y. J. et al. A high-resolution absolute-dated Late Pleistocene monsoon record from Hulu Cave China. *Science* **294**, 2345–2348 (2001).
278. Broecker, W. & Barker, S. A 190‰ drop in atmosphere's $\Delta^{14}C$ during the 'Mystery Interval' (17.5 to 14.5 kyr). *Earth Planet. Sci. Lett.* **256**, 90–97 (2007).
279. Reimer, P. J. et al. The IntCal20 Northern Hemisphere Radiocarbon Age Calibration Curve (0–55 cal kBP) *Radiocarbon* **62**, 725–757 (2020).
280. Menviel, L., England, M. H., Meissner, K. J., Mouchet, A. & Yu, J. Atlantic–Pacific seesaw and its role in outgassing CO_2 during Heinrich events. *Paleoceanogr. Paleoclimatol.* **29**, 58–70 (2014).
281. Hajdas, I., Lowe, D. J., Newnham, R. M. & Bonani, B. Timing of the late-glacial climate reversal in the Southern Hemisphere using high-resolution radiocarbon chronology for Kaipo bog, New Zealand. *Quat. Res.* **65**, 340–345 (2006).
282. North Greenland Ice Core Project members. High-resolution record of Northern Hemisphere climate extending into the last interglacial period. *Nature* **431**, 147–151 (2004).
283. WAIS Divide Project Members. Onset of deglacial warming in West Antarctica driven by local orbital forcing. *Nature* **500**, 440–444 (2013).

Acknowledgements
The authors thank L. Menviel and K. Meissner for their comments and suggestions on earlier drafts that substantially improved the manuscript. The authors also thank their Rutgers co-workers E. Hunter and R. Glaubke for drafting several figures. T.J.W. was supported by the Australian Research Council Special Research Initiative, Australian Centre for Excellence in Antarctic Science (Project Number SR200100008).

Author contributions
E.L.S., N.E.U., R.S.R. and K.A.A. researched data for the article. E.L.S. wrote the article. All authors contributed substantially to discussion of the content and reviewed and/or edited the manuscript before submission.

Competing interests
The authors declare no competing interests.

Additional information
Peer review information *Nature Reviews Earth & Environment* thanks D. Sigman, T. Guilderson, X. Ai, T. Chen and the other, anonymous, reviewer(s) for their contribution to the peer review of this work.

Publisher's note Springer Nature remains neutral with regard to jurisdictional claims in published maps and institutional affiliations.

Springer Nature or its licensor (e.g. a society or other partner) holds exclusive rights to this article under a publishing agreement with the author(s) or other rightsholder(s); author self-archiving of the accepted manuscript version of this article is solely governed by the terms of such publishing agreement and applicable law.

© Springer Nature Limited 2023

[1]Marine and Coastal Sciences, Rutgers University, New Brunswick, NJ, USA. [2]Department of Earth and Planetary Sciences, American Museum of Natural History, New York, NY, USA. [3]School of Earth and Climate Sciences, University of Maine, Orono, ME, USA. [4]Department of Earth Science, Bjerknes Center for Climate Research, University of Bergen, Bergen, Norway. [5]Graduate School of Oceanography, University of Rhode Island, Narragansett, RI, USA. [6]Department of Geosciences, University of Arizona, Tucson, AZ, USA. [7]Institute for Marine and Antarctic Studies, University of Tasmania, Hobart, TAS, Australia. [8]The Australian Centre for Excellence in Antarctic Science, University of Tasmania, Hobart, TAS, Australia.